Evaluating Electrode-Tissue Contact Force Using the Moving Pattern of the Catheter Tip and the Electrogram Characteristics

Xuyong Yu
Marquette University

EVALUATING ELECTRODE-TISSUE CONTACT FORCE USING THE MOVING PATTERN OF THE CATHETER TIP AND ELECTROGRAM CHARACTERISTICS

by
Xuyong Yu, B.S., M.S.

A Dissertation submitted to the Faculty of the Graduate School,
Marquette University,
in Partial Fulfillment of the Requirements for
the Degree of Doctor of Philosophy

Milwaukee, Wisconsin

May 2019

ABSTRACT
EVALUATING ELECTRODE-TISSUE CONTACT FORCE USING THE MOVING PATTERN OF THE CATHETER TIP AND ELECTROGRAM CHARACTERISTICS

Xuyong Yu, B.S., M.S.

Marquette University, 2019

As an important reference for the physician during catheter ablation, the electrode-tissue contact force (CF), is one of the key points for the success of the catheter ablation. With the guide of CF sensing, the ablation procedure can be much safer and more efficient.

Techniques and apparatus have been refined since catheter ablation was invented to treat cardiac arrhythmia. In the review part, different techniques for evaluating the electrode-tissue CF are discussed, including both direct and indirect measurement. Sensor-based direct measurement is broadly applied but restricted by the high cost. Surrogate markers of catheter-tissue contact such as impedance, electrogram (EGM) quality, catheter tip temperature and so on, are taken as reference evaluating CF as well, but each of them has their own drawbacks.

In this dissertation, our approach estimating the CF is based on the moving pattern of the catheter tip and electrogram characteristics. The factors determining the catheter tip motion, include the cardiac and respiratory cycles, blood flow, and so on. If the position of the catheter tip can be recorded, then the motion of the catheter tip can be tracked and analyzed. Based on our collected data, the moving pattern of the catheter tip is different when the electrode-tissue CF level varies. Features extracted from the catheter tip motion are significant for CF evaluation. There are different features selected to describe the moving pattern of the catheter tip, which are identified to best represent the movement by checking the corresponding CF as reference. In summary, if the feature has a strong correlation with the CF, then it can be taken as a good feature. Using the features as input, the CF evaluating mechanism is based on a multi-class classification decision tree to make an optimum and comprehensive estimation.

ACKNOWLEDGMENTS

Xuyong Yu, B.S., M.S.

First and foremost, I would like to express my deepest appreciation to my advisor Dr. Stephen Merrill. His constant support and encouragement have been extremely valuable to my research. This work would not have been possible without his guidance and persistent help. I am particularly grateful to him for guiding me into this exciting research area, he was not just helping me learn, but also make me a better person.

I would like to extend my sincere thanks to APN Health for supporting my work, there were lots of people providing me valuable help, especially Dr.Sra, his support and dedication to my research makes this possible. Many thanks to Dave, Mark, and Ertan, who devoted significant effort to the data collection process. I am indebted to them for their help.

I'm extremely grateful to my committee members, Dr. Rowe, Dr. Spiller, and Dr. Schmidt. They devoted significant time to my dissertation and provided me insightful comments and valuable suggestions, not only on research direction but also approaches and details. Their advice led to substantial improvement for the final work.

Last but not least, I would like to thank my family. My parents have been always supportive during my graduate study, their love and guidance are with me in whatever I pursue. Special thanks go to my loving and supportive wife, Dayeong, and my six-month beautiful baby, Cecelia, they provide me unending inspiration, bring me so much joy and happiness. I owe a great debt to them for their constant support and deep love.

TABLE OF CONTENTS

LIST OF TABLES

LIST OF FIGURES

CHAPTER 1 Introduction

1.1 Background

1.1.1 Cardiac Anatomy

The heart is located in the thoracic cavity, between the lungs and behind the left side of the breastbone. It is the organ which takes the responsibility of pumping blood through the vascular system to transport nutrients and waste products [1].

The heart wall is made of three layers: epicardium, myocardium, and endocardium. The epicardium is the outermost layer while endocardium is the innermost layer, the myocardium is located between these two, which is also the thickest layer of the heart wall, mostly contributing heart contractions. The thickness of the heart tissue is different depending on the location in the heart [1]. The internal cavity of the heart is divided into four chambers: two atria and two ventricles. Atria are the upper chambers of the heart while the ventricles are the lower ones. Atria are smaller and also thinner than the ventricles, the thickness of the heart chambers is related to the variations in the amount of myocardium present, which matters to the force generated to pump blood [2].

Heart valves are extremely important for the circulatory system. They work in coordination with each other to make sure blood flow in the right direction. On the one hand, it opens properly so that blood can pump into the next stop, on the other hand, the valves close properly so that blood cannot flow back. The tricuspid valve is located between the right atrium and the right ventricle, the function of this valve is to prevent blood from flowing back from the right ventricle into the right atrium; the pulmonary valve lies between the right ventricle and the pulmonary artery, it opens to allow blood to be pumped from the heart to the lungs where it receives oxygen. The valve located between the left atrium and the left ventricle is the mitral valve, it prevents blood from flowing backward from the left ventricle to the left atrium. The Aortic valve between the left ventricle and the aorta opens to allow blood to leave the heart from the left ventricle to the aorta and into the body [2].

Basically, the vascular system consists of two components: pulmonary circulation and systemic circulation [3]. A pulmonary circulation transports deoxygenated blood through the pulmonary veins and arteries to the lungs and return oxygenated blood to the heart [4]. Systemic circulation carries oxygenated blood from the heart through the arteries and provides nutrients and oxygen to the capillaries in the tissues of the body [5].

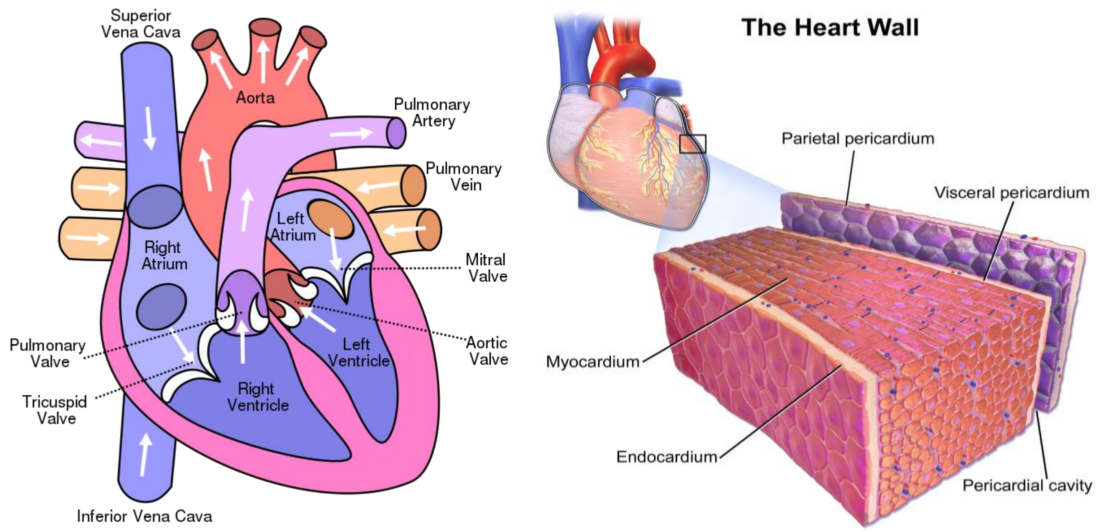

(A) (B)

Figure 1-1 The cardiac anatomy and the heart wall. (A) The photograph shows cardiac anatomy, including valves, arteries, and veins. The white arrows show the normal direction of blood flow. Image from Wikipedia: heart. (B) The photograph shows the 3D rendering showing thick myocardium within the heart wall. Image from Wikipedia: Cardiac muscle.

1.1.2 Cardiac Conduction System

The cardiac conduction system is comprised of a group of cardiac muscle cells which are able to generate and conduct electrical impulses, stimulate the heart chambers to contract and pump blood [6].

The sinoatrial (SA) node, atrioventricular (AV) node, Bundle of His, and Purkinje fibers are the major components of the cardiac conduction system. The electrical signal gets started from the SA node, which is responsible for setting the pace of the heartbeat, thus, it is also called the pacemaker of the heart. The electrical impulses from the SA node spread throughout both atria and stimulate them to contract. Later the signals travel to the AV node and there is a short delay, this delay is around one-tenth of a second, it allows the atria to contract and pump blood into the ventricles prior to ventricle contraction. After that, the signals go to the bundle of his and Purkinje fiber, stimulate the ventricles to contract [6].

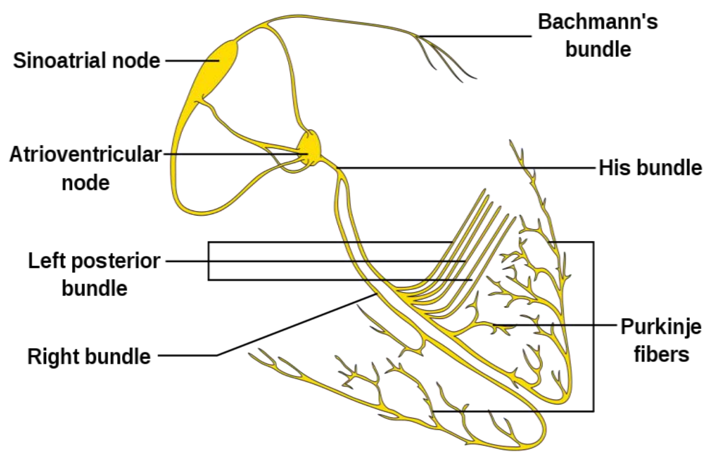

Figure 1-2 Electrical conduction system of the heart. The photograph shows the overview of the system of electrical conduction which maintains the rhythmical contraction of the heart. Image from Wikipedia: Electrical conduction system of the heart.

1.1.3 Cardiac Arrhythmias

A cardiac arrhythmia is a symptom of abnormal heartbeat which may eventually lead to heart disease, stroke or even death [7]. The beating of the heat, which is the power source of the blood circulation, critically depends on the electrical conduction, any disruptions of the normal cardiac conduction process may lead to cardiac arrhythmias [8]. Normally rhythm abnormalities can be classified as fast heart rhythms and slow heart rhythms, which are called tachycardia and bradycardia respectively. Based on the site happening in upper or lower chambers, it can be distinguished as different terminologies. For instance, Supraventricular Tachycardia (SVT), with the heart rate normally more than 150 beats a minute, starts in the heart's upper chambers while ventricular tachycardia is a fast heart rate that starts in the heart's lower chambers [9]. Atrial fibrillation (AF) is the most common cardiac arrhythmia, it is characterized by irregular and chaotic contraction of the atria [10]. In the past decade, cardiac arrhythmias are becoming a big clinical issue. Based on the data of Heart Disease and Stroke Statistics provided by American Heart Association (AHA), cardiac arrhythmias affect approximately 4 % of the population, the prevalence of atrial fibrillation (AF) ranged from around 2.7 million to 6.1 million in the United States in 2010 and it may grow up to 12.1 million in 2030 [11].

1.1.4 Arrhythmia Treatment

Some arrhythmias are normally considered harmless, which would not cause any symptom, therefore patients feel nothing most of the time. When there is a symptom like occasional extra heartbeats, the symptom would quickly disappear, and no treatment is needed. However, some of the arrhythmias may cause serious problems. For example, if a patient has an arrhythmia, which requires treatment, a doctor would need to determine whether it is clinically significant. Clinically significant arrhythmia causes symptoms or puts one at risk for complications of arrhythmias. Under this circumstance, a treatment plan would be needed for the arrhythmia.

There are several treatments have been broadly applied for arrhythmias [12][13][14]. Medication is a very common and basic treatment, and many rhythm disorders respond to medication. Even though an arrhythmia cannot be cured by medication, at least the symptoms caused by arrhythmias can be relieved by preventing episodes from starting. On the contrary, the medication may bring side effects, which may include depression and palpitations. A very common side effect of some arrhythmic medications is a slow heart rate. Medication cannot totally cure arrhythmia, but catheter ablation is a more thorough way. Catheter ablation is a procedure that radiofrequency energy or freezing are applied to destroy or isolate a specific area of the heart tissue which causes or allow abnormal heartbeats. Catheter ablation has been broadly used in the recent decades [14].

1.1.5 Catheter Ablation and Contact Force

As mentioned above, catheter ablation is a procedure to treat cardiac arrythmias by destroying a small area of the heart tissue which generates abnormal electrical impulses. The first published paper about the successful case of catheter ablation for atrial fibrillation in humans was done in 1994 in Bordeaux, France [15]. Since then, catheter ablation becomes one of the most important treatments for cardiac arrhythmia such as atrial fibrillation, atrial flutter, supraventricular, tachycardias and so on. Radiofrequency catheter and cryoballoon catheter are two of the most common catheters for cardiac ablation. Cryoballoon catheter uses nitrous oxide gas to ablate the tissue by freezing while radiofrequency catheter destroys the site by heating up the tissue. Normally, cryoablation is an alternative therapy for atrial fibrillation. In this dissertation, all the research is discussed using radiofrequency ablation. Atrial fibrillation is one of the very common cardiac arrhythmias where abnormal heart rhythm originates in an upper chamber of the heart, the pulmonary veins are called as drivers of the atrial fibrillation [16]. As a recent major treatment, pulmonary vein isolation (PVI) works well for atrial fibrillation. Wazni et al. [17] demonstrated pulmonary vein isolation is a feasible first-line approach for treating patients with symptomatic AF. Many cases are operated using catheter ablation for PVI. Radiofrequency ablation destroys the tissue generating the abnormal electrical conduction, it is a procedure to cure the arrhythmia symptom by delivering radiofrequency energy to a specific site, so it is heating up the tissue to eliminate the abnormal electrical signal. The energy is normally in the form of medium frequency alternating current in the range of 350–500 kHz [18].

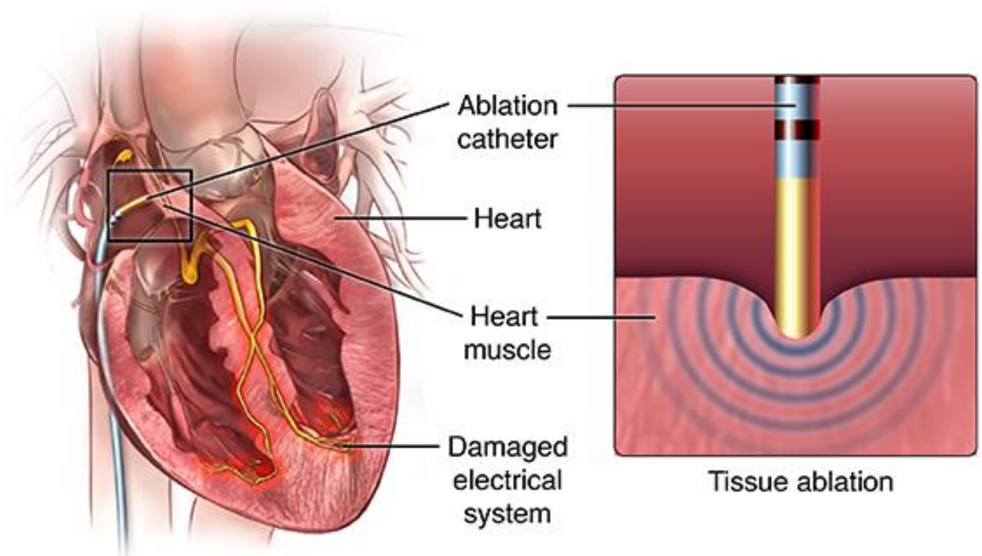

Figure 1-3 The concept of electrode-tissue contact force. The photograph shows the electrode-tissue contact during the cardiac ablation procedure using radiofrequency energy. Image from hopkinsmedicine.org.

Contact force is broadly used as a predictor for catheter ablation efficacy, it is a very important factor for the ablation safety during a catheter ablation procedure. There is a strong association between electrode-tissue CF and the resulting lesion volume during catheter ablation [19]. On the one hand, if the electrode-tissue CF is too weak, there is no guarantee to form the proper lesion size to destroy the related tissue, which causes abnormal electrical conduction, meanwhile, if the CF is too strong, it may result in cardiac complications such as perforation and tamponade occurred in all cardiac chambers. Cardiac tamponade is a medical phenomenon in which blood fills the space between the sac in the heart muscle which is severely harmful and dangerous. Yokoyama et al. [20] first emphasized the important relationship between electrode-tissue CF and lesions size in a preclinical study. Other studies [18][19] have shown that CF can predict the lesion creation and complications status using a non-irrigated ablation catheter. The significance of appropriate CF during mapping and ablation procedures have been widely recognized from the early stage of catheter ablation [21][22]. So far, no comprehensive study has been done on the cardiac perforation in the human body. However, there is some research can be found on the animal cardiac perforation. Perna et al. [23] propose a study on assessing the catheter tip CF resulting in cardiac perforation in swine atria. In their study, different locations in swine left atria and right atria are picked up to perform the perforation. The overall average CF, which cause perforation, is 175.8g ranging from 77g to 376g. Another study [24] shows the perforation force of the right atria and right ventricular is lower than that in the left atria and left ventricular. The study only performs the CF required for perforation with pigs. It might be different for human beings.

1.2 Clinical Laboratory Setup

1.2.1 Electrophysiology Lab Setup

The Electrophysiology (EP) lab provides the environment to have arrhythmia tested, diagnosed and treated. An EP study is a test to help physician's better understanding of the cardiac electrical system of the patient. If there is tissue generating abnormal signals causing arrhythmia, catheter ablation may need to be applied at the same time as the EP study. The clinical procedure of our study was carried out in Aurora St, Luke's hospital, Milwaukee, Wisconsin.

The equipment in the EP lab determines most of the design requirements. The fluoroscopy and radiography system are the basic components for the electrophysiology labs, both are applied for visualization, providing visible information for the physicians to track the process. Electrogram recording system records the signals from the surface electrocardiogram and intracardiac signals during the EP study to locate the abnormal rhythm. To make it possible to ablate the tissue which generates the abnormal signal and eliminates the arrhythmia, currently, cardiac 3D navigation and mapping system are broadly applied to guide the catheter ablation process during the EP study collecting and displaying information gathered from cardiac electrograms. Except for all these components, cardiac stimulator, radiofrequency (RF) generator, catheters, and other ablation units are also the compulsory parts for the EP lab setup.

1.2.2 Fluoroscopy System

Fluoroscopy is used to provide real-time X-ray imaging during the EP study, it is a compulsory component in the EP lab. Normally, a fluoroscopy system includes some major components such as X-ray source, image receptor, high-voltage generator, patient-support device, display device and so on [25]. The fluoroscopy system can be classified as a single plane or biplane system. The biplane system can provide accurate 3D data in real time but requires more radiation [26].

The cardiac motion can be visualized since the fluoroscopy system is able to provide continuous frames sampled at a certain rate. In our study cases, the image data was collected with 7.5 or 15 frames per second (fps).

Both X-ray dose and imaging rate are related to total fluoroscopic time during the EP study, the higher dose brings better quality image but also give more radiation to the patient. Generally, the total fluoroscopic time is one of the most important factors which determines the X-ray exposure to the patients.

1.2.3 Cardiac 3D Mapping and Navigation System

Cardiac 3D mapping system provides real-time visualization and navigation during the EP study and the catheter ablation process. In our clinical study case, Both Carto®3 (Biosense-Webster Inc, Diamond Bar, CA) and Navik 3D (APN Health, WI) are applied in the procedure.

The CARTO 3 System is an advanced technology that utilizes electromagnetic technology to generate real-time 3D cardiac map [27]. It is designed to help the physician navigate in the heart chamber by creating an accurate 3D map, pinpoint the catheter location in the chamber during diagnostic and therapeutic procedures. As for the mechanism of the CARTO 3 system, there is an ultra-low magnetic field generated by three coils in a locator pad. In the meanwhile, there are miniaturized coils placed in the ablation catheter tip. The intensity of the magnetic fields is related to the distance from the source.

Based on the strength of magnetic fields at each location of the sensor, the distance from each source coil can be determined [28][29].

Navik 3D is a newly developed system by APN Health LLC [30]. It is a cardiac mapping system that does not require any other extra specialized equipment, instead, it only relies on data generated from single-plane fluoroscopy and patient monitoring and recording systems which already present in the EP lab. 3D location of the catheter tip can be accurately measured during the procedure by applying only one view from the fluoroscopy system. The Navik 3D FDA clearance was supported by comparing the APN location result with that obtained by the Carto system, which demonstrated Navik 3D cardiac mapping system is able to accurately identify catheter locations in the heart chamber.

Figure 1-4 Navik 3D cardiac mapping system. It provides 2 user interfaces: (1) Main application generated by the system's Main computer workstation, which displays real-time fluoroscopy images and the 3D cardiac map, and (2) an interface on the Apple iPad, which serves as the controller. Image from APN Health.

1.2.4 Electrogram Recording System

An electrocardiogram (ECG) records the electrical activity of the heart over a certain time, it is broadly used for detecting heart disease and monitoring the heart's status. Normally the physician records the electrical signals collected by different electrodes, which are placed on different positions. The signals collected from the electrocardiogram allow the physician to diagnose the exact location in the heart chamber where generates abnormal impulses. Thus, the objective of the EP study is to identify the source of arrhythmias. Only if the source generating abnormal cardiac rhythm is located, there is a way to eliminate the arrhythmia.

The system for documenting the cardiac electrical signals during diagnostic and therapeutic procedures is called an electrogram recording system [31]. There are different types of EP recording systems available in the market. Though all these recording systems perform similar functions, the setup and resolution vary. The system applied in St Luke’s hospital is GE CardioLab Electrophysiology Recording System.

1.3 Statement of the Problem

CF is a force at the point of contact between two objects. For catheter ablation, it means the force between catheter tip and tissue during the ablation process. CF is an important reference for the physician because it is one of the key points for the success of the catheter ablation. With the guide of the CF sensing, the ablation procedure can be much safer and more efficient. It helps form proper lesion size during ablation and reduce the possibility of cardiac perforation and other complications.

Previously, electrode-tissue CF could not be measured directly during ablation without force-sensing ability. Physicians must estimate how much force is being applied by tactile. In recent years, techniques have been improved and there are different novel technologies have been developed to measure real-time electrode-tissue CF during mapping and catheter ablation. One of the catheters is TactiCath™ (Endosomes SA) , it uses three optical fibers to measure the microdeformation of a deformable body in the catheter tip, which correlates with tip force. Another catheter is SmartTouch® (Biosense Webster Inc), a small spring is placed between the ablation tip electrode and catheter shaft with a tiny magnetic transmitter in the tip and magnetic sensors proximal to the tip to measure the micro-deflection of the spring corresponding to tip force. The CF measurement is performed via recordings of microdeformation of a precision spring connecting the tip and the shaft of the catheter. Both CF sensing catheters have high resolution, which is less than 1 gram in bench testing and accurately display the direction of the force.

Unfortunately, these catheters are very expensive, The TactiCath catheter system consists of an RF ablation catheter, a base station, and a splitter interfacing between the catheter. The SmartTouch® catheter is a steerable 3.5-mm six-hole open-irrigated tip ablation catheter. Both catheters are placed with delicate sensors and the sophisticated structure, which makes the cost unaffordable for widely use. Thus, any technology, which could maintain the contact detection accuracy and lower the cost would benefit the application of the CF sensing.

In this study, a novel idea for evaluating electrode-tissue CF is presented based on analyzing the movement pattern of the catheter tip and the electrogram characteristics. The cost of CF evaluation can be greatly reduced because no specialized CF sensing ablation catheter is required. In the study, exploring the movement pattern of the catheter tip is the key issue, how to obtain proper features is very significant for CF evaluating. As expected, different CF level may bring different moving pattern, thus represented by different features. Generally, the features are closely related to the accuracy of the CF evaluation while the algorithm directly affects the evaluation result.

1.4 Conclusions and formulation of current studies

Cardiac arrhythmia becomes a significant problem for patients in recent decades, especially the prevalence of atrial fibrillation needs related treatment. As an effective way to treat arrhythmias thoroughly, monitoring the electrode-tissue CF during the ablation procedure has significant meaning.

In this dissertation, Chapter 2 gives a detailed introduction of the current CF measuring techniques, illustrates the advantages and disadvantages of each different technique. Chapter 3 provides a big picture of the methodology applied in the study, from the data resources to the general electrode-tissue CF evaluating system design, different features are gathered as the inputs, machine learning algorithm such as decision tree is applied to obtain the optimal evaluating result. Chapter 4 is the major part of this dissertation, which describes the details of how to extract the features from the motion of the catheter tip to evaluate CF, for the moving pattern of the catheter tip, the 3-dimensional (3D), 2-dimensional (2D) and 1-dimensional (1D) data are extracted for analysis. Chapter 5 add one additional data resource which is the electrogram for evaluating pre-ablation CF. As a supplement, the idea of electrogram comparison is proposed to demonstrate that the electrogram is related to CF evaluation. Chapter 6 is discussion and future work, discussing the work done in this project and what can be improved.

CHAPTER 2 Review of Literature

In this Chapter the historical background of electrode-tissue CF is introduced, Electrode-tissue CF is very significant for the catheter ablation procedure. Currently, there are different techniques developed for CF evaluation, including both direct and indirect measurements. These techniques are classified and elaborated in this Chapter.

2.1 Historical Background

Catheter ablation has been applied as one of the major treatments of cardiac arrhythmia over the past decades. As an important indicator of the ablation effect, electrode-tissue CF measurement has been used during ablation to ensure the procedure is safe and effective. There is some research demonstrated that electrode-tissue CF has a great impact on generating the lesion during catheter ablation [32][33][34]. Weak CF may not be able to form proper lesion size while excessive CF may result in severe cardiac complications. Before direct measurement applied to evaluate CF, there are different surrogates used to estimate the CF during the ablation procedure such as tactile feedback, visualization of fluoroscopy or ECG characteristics. Fluoroscopy provides the visualization of the catheter position which helps estimate the electrode-tissue contact in the heart chamber during the catheter ablation procedure. However, it increases the risk of radiation exposure for both physician and patients [36]. In additions, some indirect quantitative parameters such as temperature and impedance are also applied for CF evaluation [35][36].

2.2 Current CF Sensing Technologies

In recent years, there is a breakthrough which the real-time electrode-tissue contact can be directly measured by tip-tissue physical touching. In the meanwhile, with the absence of real-time CF measurement, surrogate markers of catheter-tissue contact such as catheter motion, impedance, EGM quality, catheter tip temperature and so on are also applied to estimate CF, taken as a reference during cardiac ablation. Generally, the electrode-tissue CF could be measured in different ways based on different evaluating mechanism. There are two contact sensing catheter applying different techniques are able to measure the electrode-tissue CF directly, which are also the major commercial products provided by two different companies. At the same time, there are also lots of research being done based on other characteristics as mentioned previously.

Without direct measurement, different attempts are applied to estimate the electrode-tissue contact during the catheter ablation procedure. Previously the contact force can only be estimated depends on physician experience, normally by checking the fluoroscopy and the electrogram, and tactile feedback as well during the ablation procedure. What is more, indirect parameters such as electrogram morphology, the trend of the temperature and impedance are also adopted for contact estimation [37,38]. Fluoroscopy is a very common way to monitor the catheter tip and evaluate the possible contact level, it provides the real-time visualization of the catheter tip position which is very helpful for the physician during the catheter ablation procedure, but at the same time, it may also cause the risk of radiation exposure [39,40].

2.2.1 Direct Measurement

The contact force is a direct force at the point of contact between two objects in physics area, Thus, if the contact force can be measured directly based on the physical touching, it may precisely describe the intensity of the contact. So far there are two contact sensing catheters have received FDA approval.

(1) Thermocool SmartTouch Catheter

The Thermocool SmartTouch Catheter is a newly advanced catheter to measure electrode-tissue contact force directly, developed by Biosense Webster, it gets FDA premarket approval in 2016, which is the first one to get the FDA approval in this area. The Thermocool SmartTouch Catheter enables the measurement of electrode-tissue contact during 3D mapping and ablation procedure, what is more, the orientation of the contact force can be also detected.

As for the mechanism of the contact force measurement, a very tiny spring is located in the catheter tip, which is important for sensing the contact force intensity and the orientation as well. The compression of the spring is detected every 50 ms. There are three receiving sensors located at the base of the spring which is able to transform the signal [41][42].

Contact force value, direction and the related graph are visualized on the CARTO system, which directly measures contact force continuously, providing the data in real time and allowing electrophysiologists to have an objective measure of tissue contact. This technology allows the physician to focus on electrode-tissue contact, keeping contact force at a safe yet effective level, which increases the chances of creating the transmural and durable lesions, thus, better outcomes can be achieved.

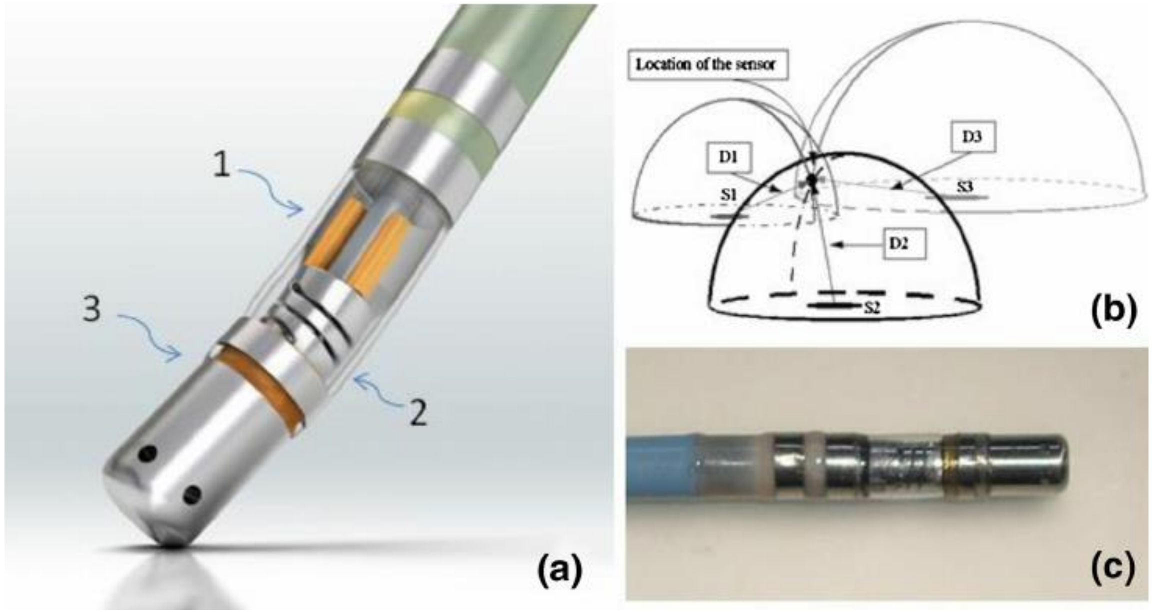

Figure 2-1 The Thermocool SmartTouch CF catheter is the first FDA approved CF sensing catheter. A small spring coil connects the tip electrode to the catheter shaft. A magnet signal emitter is located distal to the spring. Three magnetic location sensors, positioned just proximal to the spring, measure the microdeflection of the spring to compute the force magnitude and angle on the tip electrode. Reproduced, with permission (a) shows the basic structure of the catheter (b) shows the detailed design (c)shows the general looking. Image from ResearchGate

The SMART-AF trial [43] is a multicenter, nonrandomized, prospective study, which is carried out to evaluate the safety and effectiveness of the ThermoCool SmartTouch contact force sensing catheter during the catheter ablation. Totally there are 172 patients from different sites got involved in the study, who had failed the medication treatment before, except for some roll-in patients, eventually there are 160 patients took the catheter ablation procedure, for the safety checking, any adverse events including tamponade, heart block, vascular access complications and so on are all counted which occurred with the first 7 days after the procedure. For the effectiveness validation, the result shows that a 12-month free from the atrial fibrillation/atrial.

After Thermocool SmartTouch Catheter has been developed, there are several studies examining the benefit brought by the newly emerged CF sensing technique. Lee et al. [44] showed that applying Thermocool SmartTouch catheter reduces fluoroscopy time by 77%, radiation dose by 71%, in the meanwhile, total procedural time is decreased by 19% during catheter ablation.

Pulmonary vein isolation (PVI) is a very common treatment for atrial fibrillation, with the guidance of the contact force measurement system provided by SmartTouch catheter, it affects procedural parameters such as fluoroscopy and procedural times, make the operation more efficient without significantly increasing complications, what is more, continuous contact force monitoring in real time during ablation gives more support to the physician and it is helpful for data statistics as well [45][46][47].

Except for the magnitude and duration of the contact force during ablation, the quality of electrode-tissue contact also affects the ablation efficacy. Generally, the contact force is affected by multiple factors, including atrial rhythm, contact orientation, catheter navigation mode and so on [47].

(2) TactiCath catheter

In 2008, the paper “Novel contact force sensor incorporated in irrigated radiofrequency ablation catheter predicts lesion size and incidence of steam pop and thrombus” [20] first brings up the idea of applying optical characteristics for evaluating contact force. TactiCath catheter (Endosense, St. Jude Medical, St. Paul, MN, USA) is an open-irrigated radiofrequency catheter, it was developed to measure the real-time electrode-tissue CF, which is also the second FDA-approved CF-sensing catheter. There are three optical fibers attached with fiber Bragg gratings (FBG) to a deformable body. The infrared laser light generated from the system can travel along the TactiCath catheter all the way to the tip, the light with a specific wavelength can be reflected back towards the source [48]. When there is contact between the catheter tip and tissue, the cavity length changes, which affect the pattern of the reflected wavelength of the light. By checking the reflected wavelength of the three optical fibers, the contact force can be evaluated since it is proportional to the change of the reflected wavelength. The magnitude and the orientation of the electrode-tissue contact force are calculated at intervals of 100 ms, which is able to provide real-time contact force evaluation [48][49][50].

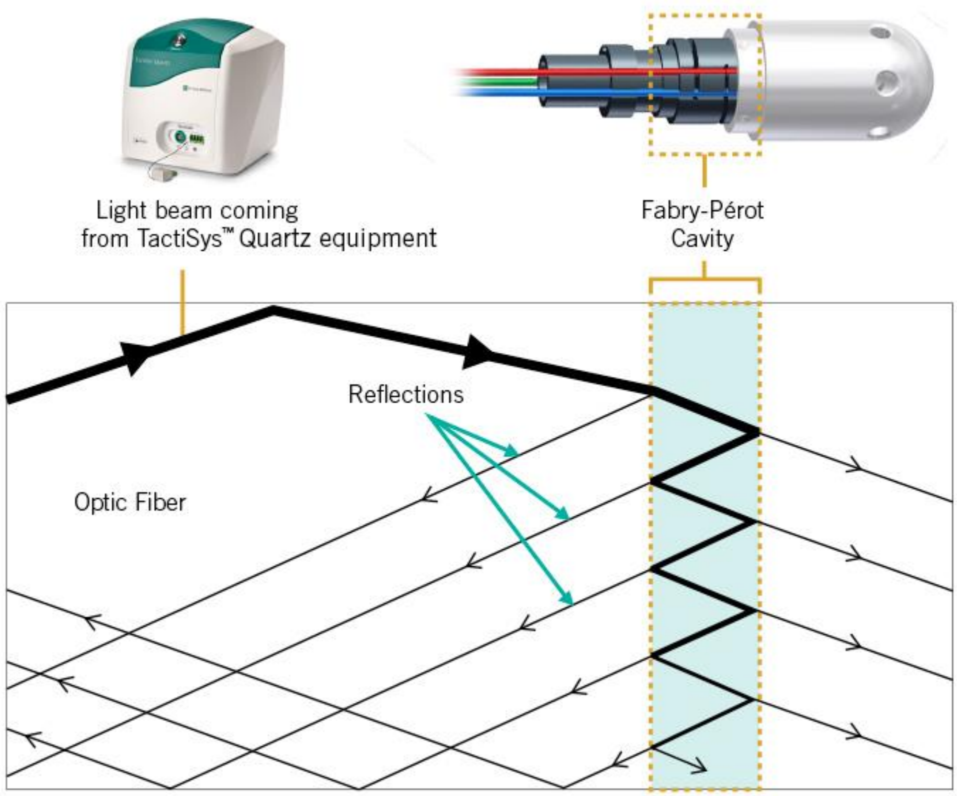

Figure 2-2 The TactiCath catheter has a sensor at the catheter tip which is based on a Fabry-Perot interferometer, evaluate CF based on optical characteristics. Image from St. Jude Medical.

The TOCCASTAR trial [51] is a prospective, multicenter study, it was carried out to determine the relationship between catheter contact force and clinical recurrences during follow-up. What is more, the clinical study result also makes the TactiCath CF sensing catheter gain FDA approval. Totally there are 32 patients with paroxysmal AF taking the procedure by using the TactiCath CF sensing catheter, after the treatment the patients were followed for 12 months.

During the study, different levels of CF were applied, 35% of the applications were carried out with an average CF of 10 g. Based on the observation, all the patients treated with this low CF experienced recurrences, on the contrary, no recurrence for 80% of the patients who were treated with an average CF of 20 g during the ablation procedure within12 months. What is more, the study also shows that 75% of the patients treated with 500 gs of the average FTI were recurrent, however, there is only 31% treated with 1000 gs had recurrences. The study [48] shows that the contact force measurement is quite accurate based on this mechanism. Moreover, they confirm contact force is a major determinant of radiofrequency lesion size as well. in the meanwhile, steam pop and thrombus incidence also increase with contact force. Based on this specified working mechanism, the TactiCath ablation catheter has been developed by Endosense SA as a commercial product.

2.2.2 Indirect Measurement

The CF sensing catheters can directly measure the electrode-tissue CF, however, they are very expensive and not affordable for all the scenes, The TactiCath catheter system consists of an RF ablation catheter, a base station, and a splitter interfacing between the catheter [48]. The SmartTouch catheter is a steerable 3.5-mm six-hole open-irrigated tip ablation catheter [41]. Both catheters are placed with delicate sensors and the structure is sophisticated, which makes them unfordable for widely use. Thus, any technology, which could maintain the contact detection accuracy and lower the cost would benefit the application of the CF sensing.

(1) Evaluating contact force by impedance

Impedance is a useful surrogate maker to evaluate the CF, it has been suggested as an effective indicator of electrode-tissue contact [52].

Impedance and catheter contact are strongly related, Strickberger et al. first explored the relationship between impedance and electrode-tissue contact during radiofrequency catheter ablation, they found the impedance is 22% greater when there is a strong contact between the endocardial and catheter tip compared with a weak contact [53]. Another study predicted the insertion depth of the catheter tip into the endocardium by utilizing the impedance between the dispersive electrode and the ablation catheter electrode, which demonstrated that the impedance is an effective indicator for predicting electrode-tissue contact during cardiac catheter ablation [54].

There is a significant correlation between the linear lesions size and pre-ablation impedance, the pre-ablation impedance could be applied as an indicator for the creation of long, continuous, and transmural linear lesions with a multi-electrode catheter [55].

Tissue heating during RF catheter ablation results in an impedance fall at the catheter tip. When greater electrode-tissue contact force is applied during RF catheter ablation, the initial impedance fall is also larger [56], Thus, monitoring of the initial impedance fall can be applied as an indicator of catheter contact to improve ablation lesions formation. Impedance drop during the catheter ablation has a strong correlation with lesion formation, which is a very reliable indicator of the ablation effect. Tobias Reichlin et al. proposed a study demonstrated that ensuring impedance fall during catheter ablation is a successful strategy to achieve the ablation goal for atrial fibrillation [57]. Another study demonstrated that contact force correlates with impedance fall during 60 seconds of radiofrequency ablation. When the contact force is greater than 5 g, it brings greater impedance fall, but if over 20 g may lead to tissue overheating problem later [58].

(2) Evaluating contact force by tip temperature

Temperature is a very significant factor during cardiac ablation. When the radiofrequency energy is delivered through the electrode, its temperature goes up and the energy is conducted to the tissue, thus the temperature of the ablation site increases as well. Thus, if it has good energy delivery between the catheter tip and tissue, normally the temperature increases a lot. Basically, lots of related technologies for sensing the temperature takes advantage of the related phenomenon to verify the electrode-tissue contact.

“Cardiac ablation systems and methods using tissue temperature monitoring and control” [59] by Roger A. Stern et al. in 1998, were granted a patent for a cardiac ablation system which applies temperature sensing element measuring the temperature of the tissue during an ablation procedure. “Sensing contact of ablation catheter using differential temperature measurement” [60] by Assaf Govari et al. in 2014, were granted a patent for providing a medical apparatus which includes two temperature sensors, one disposed on the distal portion sufficiently proximate the ablation electrode to measure the temperature during ablation procedure while the other one placed on the distal portion sufficiently distant from the ablation electrode to be less able to detect the heat. generally, the mechanism of this apparatus based on the temperature difference during catheter ablation when part should be hotter in contact with tissue while the part in contact with blood. “ablation catheter electrode having multiple thermal sensors and method of use” [61] by Wang et al. in 2013, propose an apparatus which the electrodes contain three thermal sensors located in different positions in the electrode which are able to detect temperature differences on the surface of the catheter tip. Basically, the temperature is an important indirect surrogate which shows the contact between the catheter tip and tissue, nowadays applying more thermal sensors seems becoming a trend.

(3) Evaluating Contact force by EGM characteristics

EGM records the electrical activity of the heart using electrodes implanted in the heart [31]. Normally, the physicians always check the EGM during catheter ablation to ensure the ablation energy is properly delivered, especially the signal from the ablation catheter electrode can be taken as an important reference. Kumar et al. [62] propose a study to evaluate contact force by electrogram characteristics, several features are applied as follows: (1) Total, positive, and negative EGM amplitude. (2) EGM width. (3). EGM morphology such as QS, QR, QRS, etc. (4) Percentage reduction in the EGM amplitude with ablation. Data is collected to show the correlation between the contact force and EGM amplitude/width, but eventually it was demonstrated that just a moderate to poor correlation between contact force and EGM amplitude and EGM width, but as they claimed, EGM characteristics can be applied as an important reference during catheter ablation.

Ullah et al. [63] described the impact of catheter contact force left atrial electrogram characteristics. Their work shows that changes in electrode-tissue contact force and the orientation both would affect the electrogram characteristics, not only the electrogram magnitude but also morphology.

2.3 Impact of the Electrode-Tissue CF

The contact force is very significant for estimating radiofrequency ablation efficacy. More importantly, it is also an important factor for the safety profile during the catheter ablation procedure.

Before contact force measuring technique invented, there was research exploring the relation between lesion generation and some related surrogates such as temperature and impedance, Avitall et al. [64] proposed a study finding impedance decrease is highly correlated with temperature increase, which can be used as a predictor of the electrode-tissue contact. Yokoyama et al. [20] first emphasized the important relationship between the electrode-tissue contact force and lesions size in a preclinical study. It has also been proved that the lesion size increases strikingly when contact force increasing. When CF is increased from a low CF to high CF, the lesion depth is increased by 70% at 30 Watts and by 90% at 40 Watts [65]. FTI is a time-variant measure of CF, it has been identified that both FTI and contact force are correlated with lesion formation, FTI correlates linearly with the lesion depth and volume despite constant RF power delivery and identical peak contact force [66]. Another study [67] shows that during radiofrequency delivery, a target FTI of 392 gs can be used as an endpoint for each ablation site.

So far, no comprehensive study has been done on researching the cardiac perforation in the human body, but there is some research can be found in animal cardiac perforation [24,68,69,70]. Perna et al. [23] propose a study on assessing the catheter tip contact force resulting in a cardiac perforation in swine atria. In their study, different locations in swine left atria and right atria are picked up to perform the perforation, the overall average contact force which causes perforation is 175.8 g, ranges from 77 to 376 g. Another study [24] shows that the perforation force of the right atria and right ventricular is lower than that in the left atria and left ventricular, what is more, with the ablation catheter in the sheath, left ventricular perforation is achieved more rapidly. The contact force required for perforation should be different for human beings compared with pigs, but their studies provide some useful information as a reference.

the EFFICAS I study [71] is significant which gives the optimal contact force recommendation of 20 g and FTI at least 400 gs for the ablation spot. During the ablation procedure, the CF information is not provided to the physician. There is a diagnostic procedure performed to evaluate the gap location as correlated to index procedure ablation parameters. In total, there are 26 out of 40 patients showed 1 gap. Ablations with a minimum FTI less than 400 gs showed an increased likelihood for reconnection. Thus, they conclude the reconnection is strongly correlated with CF and FTI at the site of a gap. The EFFICAS-II trial [72] is a continuation study of the EFFICAS I study. It was carried out to validate the parameters and the related results posted in EFFICAS-I. Based on their results, by using the TactiCath catheter with the CF of 20 g and FTI greater than 400 gs, three months after the PVI treatment, there are 24 patients returned for assessment. At follow-up, 85% of PVs treated with CF guidelines were chronically isolated.

CHAPTER 3 Methodology

This Chapter gives an outline of research methods that were followed in this study, which focuses on data collection, feature selection, and the construction of CF evaluating system. Data collection describes the data resources and the details of collecting data in this context. Some features extracted from the movement of the catheter tip and electrogram characteristics are selected as inputs for the CF evaluating system, which produces an estimate of the CF. The proceeding of feature selection will be illustrated in the next Chapter. Based on the input and output, the construction of the CF evaluating system will be discussed in Section 3.2.

3.1 Data Description

3.1.1 Data Resources

The data resource in our clinical studies includes three parts: one is fluoroscopy data, containing the catheter tip location information; another one is intracardiac electrogram data collected by EGM recording and monitoring systems; the last part is CF data collected using the ThermoCool® SmartTouch® system.

(1) Fluoroscopy

Biplane fluoroscopy is one way to obtain the 3D location of the catheter tip in the study. It can precisely locate the 3D position of the catheter tip using the back-projection algorithm [73], it reconstructs the 3D position by taking the 2D position from each view. Normally the first step is to find and record the tip's 2D location in every frame. The second step is running a back-projection calculation for each pair of the 2D tip locations from the two different views. Thus, the frame-level 3D position of the catheter tip can be obtained.

Normally a single plane fluoroscopy facility is very common in the EP lab but only provides 2D catheter information. There is research being able to identify the third dimension in 2D fluoroscopy to create 3D cardiac maps, but most commonly, biplane fluoroscopy provides the 3D location more accurately which we call it ground truth. The biplane fluoroscopy setting depends on the lab condition. For the clinical data collected in this dissertation, biplane fluoroscopy is applied for getting the accurate 3D catheter tip data for some of the datasets.

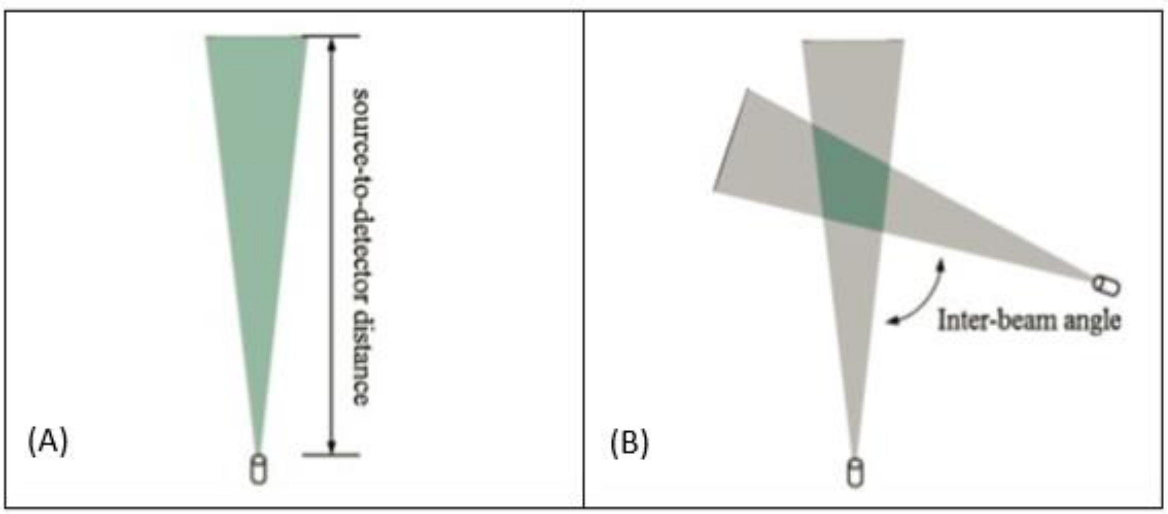

Figure 3-1 Biplane fluoroscopy using different views. (A) A perspective projection model of the single-plane fluoroscopy with a certain source-to-detector distance. (B) A perspective projection models for the biplane fluoroscopy with a certain inter-beam angle. Image from Wikipedia: Cardiac muscle [73].

Cardiac mapping systems provide another way to obtain the catheter tip location during the EP study. Cardiac mapping systems employ different catheter locating techniques. For instance, the CARTO system functions by using magnetic localization technology to determine the catheter tip location. There are ultralow-intensity magnetic fields emitted from coils in a location pad beneath the laboratory table, which can work with the sensors incorporated in the catheter tips, allows the CARTO system to precisely localize, record, and display the position of the catheter tip in real time, not only in three dimensions (*x*, *y*, *z*), but also the orientation [74].

Navik 3D is the first cardiac mapping system that does not require specialized equipment to interface with the patient, it gives the physician a real-time 3-D catheter location in the heart from the 2-D fluoroscopic images. Single plane fluoroscopy only provides the 2D view to the physician, which means it is only possible to view the catheter location along the X-Y plane, but the Z-axis is not discernible. In the Navik 3D cardiac system, based on the size of the tip projection, the location for z-axis can also be calculated to create the complete 3D data with high accuracy. For some of the clinical study cases in our study, the data resource for discovering the moving pattern comes from this way, which uses Navik system and single plane fluoroscopy to get the catheter tip location [30].

(2) Electrograms

Electrograms come from two different sources: surface electrocardiogram (ECG) and intracardiac electrograms (EGM’s). Surface ECG is the process of recording the electrical activity of the heart using different electrodes placed on different body parts during a certain period, while EGM’s is obtained by electrodes placed within the heart via cardiac catheters. In our study, EGM’s signals coming from 16 channels are documented in real time during diagnostic and therapeutic procedures. What we can see from the monitoring system is the analog signal. In the EGM recording system data is saved in the digital form with a certain sampling rate. Thus, the overall magnitude and direction of the heart's electrical depolarization are captured at each moment throughout the cardiac cycle. Figure 3-2 shows an electrogram record.

Figure 3-2 Two-lead body surface ECG (top 2 channels) and cardiac EGM of Abl, Abl p, RA, CS p, CS d in a patient. Image from Clinical Electrophysiology Review, Chapter 6: Catheter Ablation

(3) Contact Force (CF)

The Thermocool® SmartTouch® Catheter is a newly advanced catheter to measure electrode-tissue CF directly. It enables the measurement of electrode-tissue contact during 3D mapping and ablation procedure. Moreover, the orientation of the CF can also be detected. The force and contact information are graphically displayed on the Carto 3 Mapping and Navigation System with the Carto 3 SmartTouch® Software Module. In our study, the CF collected by SmartTouch® Catheter is used for reference.

3.1.2 Data Collection

(1) 3-dimensional data collection

There are two different ways to get the 3D data in our study. One is using biplane fluoroscopy to generate 3D data using the back-projection algorithm, firstly the catheter tip location from the 2D view is extracted and the 3D position is computed later. The other way is using Navik cardiac mapping system to record the 3D position of the catheter tip during the ablation procedure, but it is not frame-level 3D data, which means the time series of the 3D catheter tip location is not complete, some of the frames are missing.

(2) 2-dimensional data collection

The 2D data can be extracted from the obtained 3D data, normally by the projection of the 3D data on some specific direction, more details of the 2D data extraction will be introduced in the next Chapter. The AP view and lateral view showing the 2D images also provide some straightforward 2D data, which for some part in the research is also used.

(3) 1-dimensional data collection

1D data is also extracted using 3D data. The 3D data incorporates the X, Y, Z coordinates of the catheter tip position, the data from the three directions can be extracted to form a time series. Time series is a sequence of measurements over time. In our case, it is the tip position measurement from X, Y or Z component over time.

(4) Electrogram data collection

The electrogram data is documented by the electrogram recording system, in our study, 16 channels from the intracardiac electrogram are provided on the monitor and recorded as well. My interest focuses on the signal from the ablation distal electrode and the reference electrode, which normally is the Cs p electrode taken by the physician, more details will be revealed in the next Chapter.

3.2 Research Design

3.2.1 The Features Extracted from the Moving Pattern

The research gets started with exploring what kind of features can best represent the moving pattern of the catheter tip. The electrode-tissue contact has an impact on the moving pattern of the catheter tip, which is one of the conclusions in this research. The moving pattern can be described using some features that best represent the moving character. In this dissertation, three different features are selected to describe the moving pattern of the catheter tip as follows:

(1) 3D distance (The average distance of the points to the fitting plane)

(2) 2D ratio (The ratio of the long axis and short axis of the projected 2D points)

(3) 1D cost (1D time series similarity comparison)

Based on the data collected in our study, these three features will be demonstrated to be related to the CF in Chapter 4. Each feature is analyzed respectively at the beginning. Eventually, all the features are combined to make a comprehensive prediction since no single feature can best represent the CF. As for exploring and adding more features to evaluate CF, the answer should be positive. If there are more features found can nicely represent the moving pattern of the catheter tip, the CF evaluating system can incorporate them and take it as input.

3.2.2 The Features Extracted from the Electrogram

Except for the moving pattern of the catheter tip, the electrogram data is also collected for research. The contact between the electrode and tissue is demonstrated to be related to the electrical coupling. In this study, the signal from the frequency domain is used to explore the relationship between the CF and electrogram characteristics. There is a limitation of using the electrogram to predict CF during catheter ablation, one important reason is that if the tissue is ablated, then the CF is not the dominant factor determining the electrical coupling anymore, this will be explained in Chapter 5. On the contrary, as additional information for contact force estimation, the characteristics of the electrogram can be very effective surrogates for pre-ablation CF evaluation.

3.2.3 An Overlook of the CF Evaluating System

As a CF evaluating system, there should be input, output and the evaluating mechanism. The collected data needs to be processed to obtain the input. As mentioned before, three different features are selected as inputs. To get the input of the CF evaluating system, the whole procedure can be classified into three stages. The first stage is data collection which has been introduced in the previous section. The second stage is feature selection, based on collected data, some features are extracted, which is crucial for describing the catheter tip moving pattern properly. The final output of the CF evaluation is divided into four ranges: strong, good, medium, low. CF evaluating mechanism is based on a multiclass classification decision tree, taking different features as input, eventually getting the output of a CF range, more details will be introduced later.

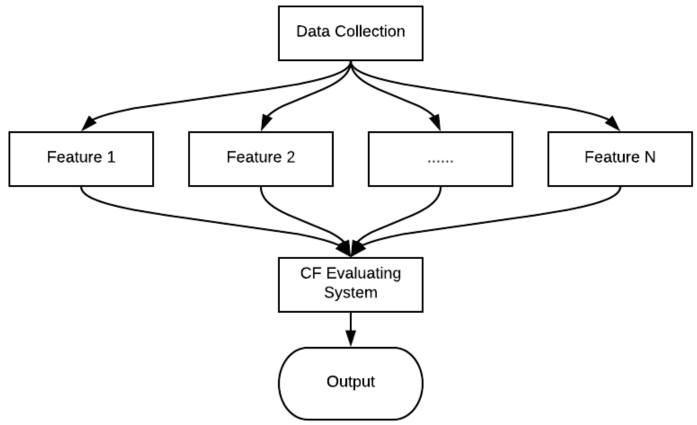

Figure 3-3 A general structure of the CF evaluating system.

3.2.4 Input of the CF Evaluating System

Input is based on data collection. Before the procedure gets started, obtaining a tip position is required. This part is processed by the cardiac mapping system or biplane fluoroscopy using the back-projection algorithm, which both are able to provide the tip location during catheter ablation. Moreover, the electrogram data is also collected as input.

The moving pattern of the catheter tip is different when the electrode-tissue CF level varies. The features extracted from the catheter tip moving pattern are required to describe the difference. For example, the 3D coordinate of the catheter tip during radiofrequency ablation can be obtained, which is a sequence in a 3D space within a period of time. Based on observation, we will show that if the CF is stronger, there is a high possibility that all the points gathered tightly fitting on one surface. What is more, the average distance of each point to the plane we can take it as the feature, the 3D distance is less, there is a greater probability that the CF is stronger. Otherwise, there might be weaker contact.

Feature selection is significant for CF evaluation. If the feature has a strong correlation with the CF, then it can be taken as a good feature. The example mentioned above, which is the average distance of the points to the fitting plane in the 3D space, suppose that distance gets smaller when the CF gets stronger, gets greater when the CF gets weaker, then it would be perfect for CF evaluation.

In our study, 3D distance, 2D ratio, and 1D cost as mentioned above are selected as input. The value is computed in the form of continuous numbers but later they are separated into ranges which become discrete values. The details of how to extract the features and the correlation between the features and CF is discussed in Chapter 4.

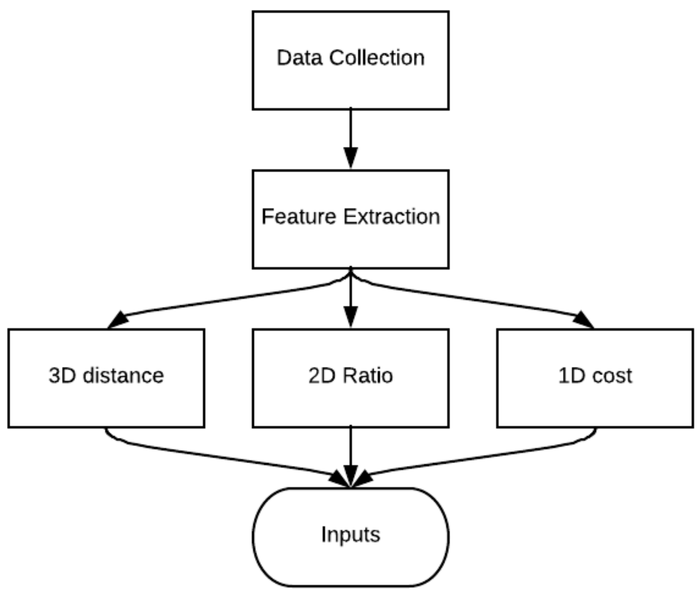

Figure 3-4 The components of the CF evaluating input.

3.2.5 Output of the CF evaluating system

The output of the CF evaluating system is the CF contact level, which is separated into 4 levels: strong, good, medium, weak. Weak CF during cardiac catheter ablation means the contact needs to be enhanced by the physician, medium CF can be used for ablation but not perfect, good is the best level while strong means too much, which may cause perforation or other adverse effects.

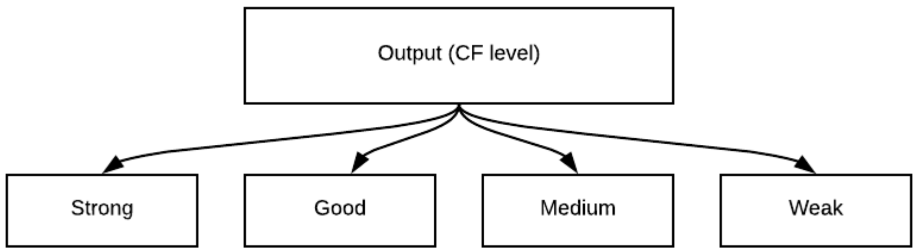

Figure 3-5 The range of the CF evaluating output.

3.2.6 CF Evaluating System Construction

The CF evaluating mechanism is based on machine learning, there are different algorithms working for the evaluation mechanism. Considering the data size and the output range, a decision tree is a good way to describe it. As for the decision tree, based on the difference of the splitting mechanism, it can be classified as Gini index-based decision tree and entropy-based decision tree [75][76]. In this study, the entropy-based decision tree is adopted for classification.

(1) Entropy-based Decision Tree

Entropy originates from the information theory. If there is more information in the dataset, the entropy is higher, on the contrary, the entropy is lower. It is used to measure the level of impurity in a group, which can be defined as following, P_i is the probability of class i.

$$Entropy = \sum -p_i(\log_2 P_i) \tag{3.1}$$

For a binary decision tree, there are only two classes, which is the most common case for the decision tree implementation. The entropy is computed using only two items.

$$Entropy = -p(a) * \log_2 p(a) - p(b) * \log_2 p(b) \tag{3.2}$$

Suppose all the samples are from the same class in the datasets, the value of the entropy should be 0. If it is evenly distributed in either class, then the entropy value reaches the maximum value which is 1. For a two classes case, we can see a basic trend of the entropy in Figure 3-6 below. The entropy is maximum when $p = 1/2$, which means each class takes half in the datasets. The entropy reaches zero which is the minimum when probability is $p = 1$ or $p = 0$, which indicates only one class in the datasets, the entropy is the lowest at this moment.

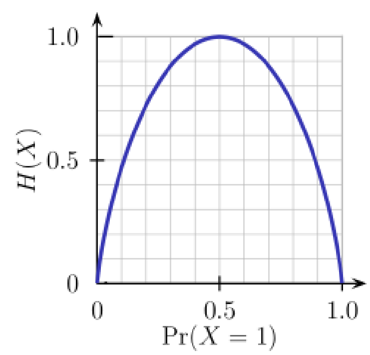

Figure 3-6 The binary entropy function. the entropy is zero when probability is p=1 or p=0. The entropy is maximum which is 1 when the probability is p=1/2.

We want to determine which attribute in a given set of training feature vectors is most useful for discriminating between the classes to be learned. Information gain tells how important a given attribute of the feature vectors is. Information gain is used to decide the ordering of attributes in the nodes of a decision tree.

A decision tree consists of three types of nodes [76]: root node, internal nodes, leaf nodes, each leaf node is assigned a class label. The non-terminal nodes, which includes the root and other internal nodes, contain attribute test conditions to separate the records. For building a decision tree, there is an attribute condition test on each non-terminal node and each terminal node is a classified label. Basically, each node represents a test performed on a single attribute and go left or right depending on the result of the test. Then keep traversing the tree until we reach a leaf node which contains the class prediction. In total, there are two steps for applying a decision tree for binary classification:

- Attribute selection

The first step is determining what attributes of the data are relevant to the target class want to predict, which is also called attribute selection.

- Constructing a decision tree

Finding the attribute that best splits the target class into the purest possible children nodes. Thus, a normal way that is about information gain based on entropy is applied to solve this problem.

(2) Decision tree for CF evaluation

A basic decision tree has only two labels. In our study, for combing the different features, a basic decision tree is adopted firstly to make an analysis. The first step for building a decision tree is set up the attributes and classes. Three features are selected as the attributes mentioned above already. The classes are the CF ranges, for the two-class case, the four ranges are decreased to two which just generalize the CF to be good or bad.

The three attributes which are the inputs for the CF evaluating system are obtained with a specific value before processing, but in the decision tree, it is simplified as a certain range. 3D distance and 2D ratio are summarized as “big’, “medium”, “small” to describe the value, while time series similarity is summarized as “similar” and “dissimilar” just to describe the one-dimensional time series similarity level. As for the CF range classification, the goal of the computation is keeping running all the attributes to get the greatest information gain at each node and pick up that specific attribute for the node. At each node of the tree, this computation is performed for every attribute, and the feature with the largest information gain is chosen for the split in a greedy manner. A two-class decision tree is the basic component for the following multiclass decision tree. More details about the attributes and the quantization will be described in Chapter 4.

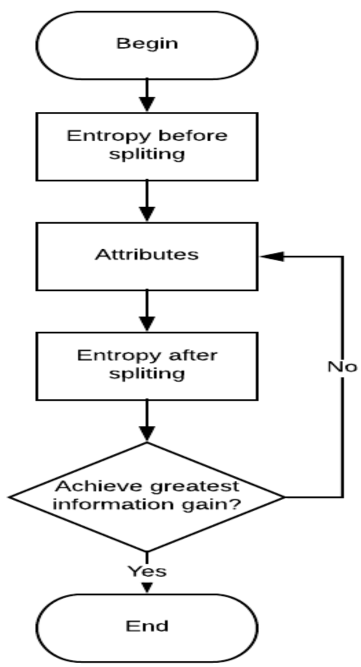

Figure 3-7 The process of splitting the attributes

(3) Multiclass Classification Decision trees

A decision tree provides the output of “strong” and “weak” for CF evaluation, which is not delicate enough for requirement during catheter ablation. Thus, multiclass classification is applied to obtain a more accurate CF level classification. The difference between binary and multiclass classification can be simply described as [77]:

- Binary classification: Y = {0, 1} which only has two classes
- Multiclass classification: Y = {0..., K-1} which has K classes

Actually, a multiclass classification decision tree is built based on a binary decision tree [78,79]. There are different forms of combinations as following:

- One VS One, suppose there are N classes, then $\mathrm{N}(\mathrm{N}-1)/2$ binary trees are required, each tree generates one result, eventually, all the result will be summarized to pick up the biggest value.
- One vs Rest, Only N classifiers are required.
- Many VS Many.

In this study, the first combination is applied for classification. The goal of multiclass classification decision trees is to learn to classify K classes correctly. Following the previous procedure, the structure of the multiclass classification decision tree is as follows. There are 6 different decision trees considering there are 4 classes as output, the amount of the decision tree is $\mathrm{N}(\mathrm{N}-1)/2$, N is the number of the classes.

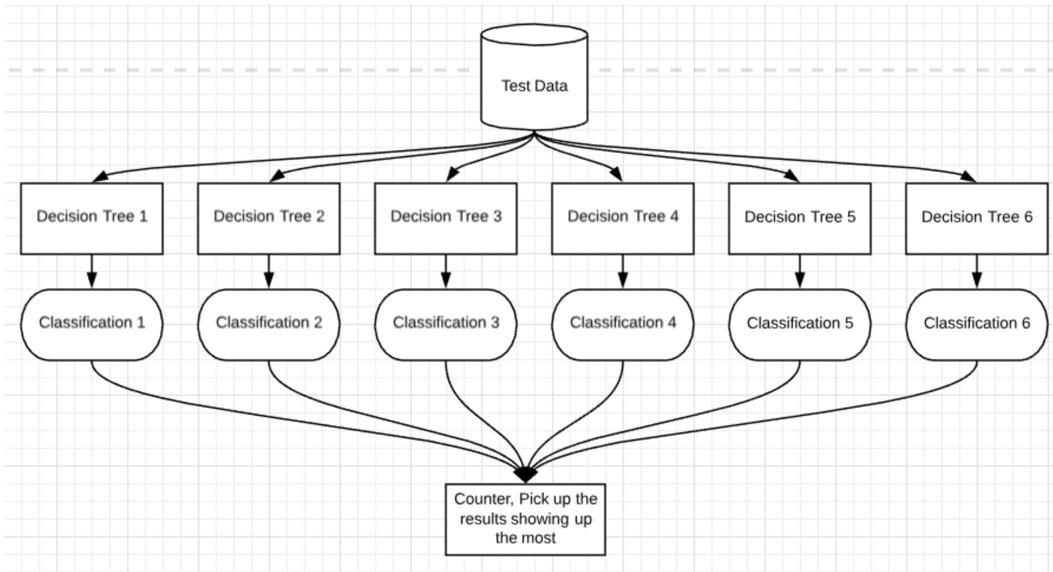

Figure 3-8 The multiclass classification decision tree in this study

The final output of the CF evaluation is divided into four parts: strong, good, medium, weak. The combination includes “strong-good”, “strong-medium”, “strong-weak”, “good-medium”, “good-weak”, “medium-weak” since the mode of “One vs One” is adopted for multiclass classification,

After all the binary decision trees are built, the multiclass can be classified using the input data. Each tree runs the data and gets one output. The process is just like voting, the CF level is determined by the output that gets the highest votes.

3.3 Summary

There are several important issues for constructing the CF evaluating system. Data collection is the basis for further processing, in the meanwhile, feature extraction has a great impact on the result.

This Chapter focused on data collection, feature selection, and the CF evaluating system. Data collection describes the data resource and the details of collecting data. Some features are selected as input for the CF evaluating system after processing the collected data. The feature selection will be illustrated in the next Chapter. Based on the input and output, the mechanism of the CF evaluating system is discussed using a multiclass classification decision tree.

CHAPTER 4 The Moving Pattern of the Catheter Tip and the CF

In this Chapter, there are several features extracted using the motion of the catheter tip during the catheter ablation procedure, which is demonstrated to relate to the CF. In order to get a comprehensive analysis and more accurate prediction, different features are combined for CF evaluation.

4.1 Moving Pattern of the Catheter Tip

A catheter tip is not still during catheter ablation. The factors determining the moving pattern of the catheter tip, include the cardiac and respiratory cycles, blood flow, and so on. If the position of the catheter tip can be recorded, then the moving pattern of the catheter tip can be tracked and analyzed.

There are different ways to obtain the catheter tip movement data during catheter ablation. With fluoroscopy data, normally certain frames are recorded at 7.5 or 15 frames per second (fps). The 2D position of the catheter tip can be obtained using image processing technology. 3D position can be generated applying cardiac 3D mapping system. As mentioned, Navik uses real-time images from 2D fluoroscopy and the geometry to identify the 3D position of the catheter tip. What is more, biplane fluoroscopy is able to provide 3D catheter tip position as well; Carto® 3 is another cardiac mapping system which is broadly used for catheter ablation. Therefore, by all these means, the movement of the catheter tip in 3D space can be observed based on the fluoroscopic data. This process results in a sequence of 3D catheter tip positions. In my dissertation, I assumed that the movement of the catheter tip is related to electrode-tissue CF. The tip movement pattern might be more random when electrode-tissue CF is weak, more regular when CF is strong.

4.2 Three-Dimensional Data Analysis

4.2.1 Catheter Tip 3D Data Description

When the movement of the catheter tip is depicted in a 3D space, the moving pattern can be analyzed by the catheter tip motion. In X, Y, Z coordinates, the track of the catheter tip is discrete, since there is a certain frequency to make the measurement depends on the facilities. For a biplane system, the sampling rate is the same as the fluoroscopy frame rate.

The physician places a catheter tip at a certain position in the heart chamber to obtain the spatial information during the mapping process in a clinical study case. The following graphs show the AP view and Lateral view respectively using biplane fluoroscopy, Figure (A)(B)(C) are three consecutive frames from AP view while (D)(E)(F) are the counterpart frames from the lateral view. From each frame, the 2D catheter tip position can be located and 3D position can be extracted by the back-projection algorithm. In Figure (G), the 3D position of the catheter tip in all the frames is gathered in a 3D space.

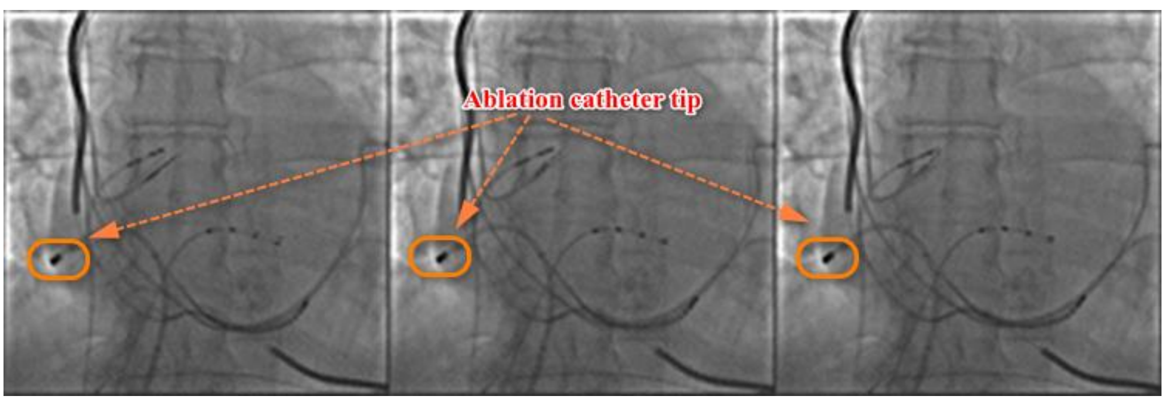

(A) (B) (C)

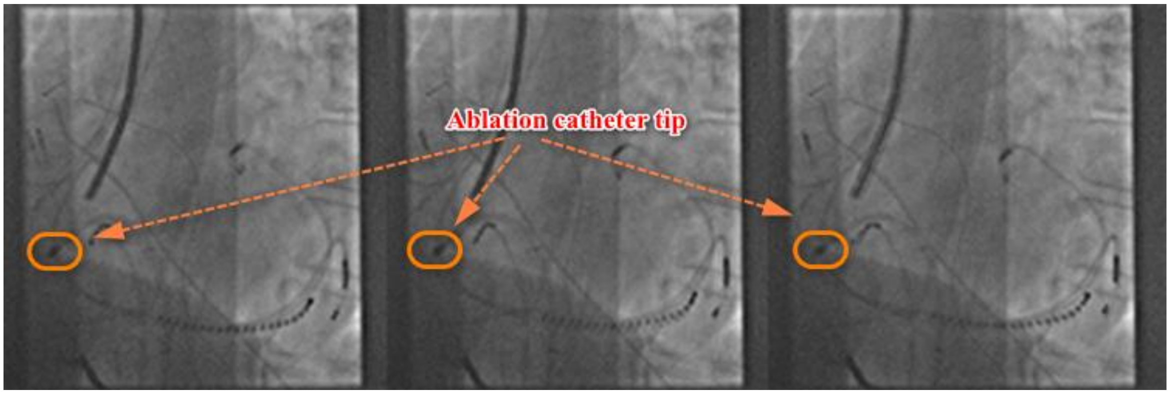

(D) (E) (F)

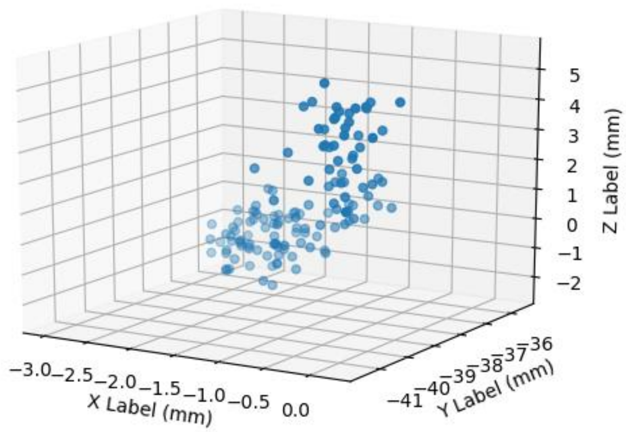

(G)

Figure 4-1 Catheter tip 3D location data description. The 3D location data of the catheter tip can be generated using the biplane system with back-projection algorithm applied. (A)(B)(C) three consecutive frames from AP view. (D)(E)(F) three consecutive frames from LAO view. (G) 3D points of the catheter tip from different frames in a 3D space.

4.2.2 The Idea of Surface Fitting

With the monitoring of the fluoroscopy system, the 3D position of the catheter tip in the heart chamber can be located. During the mapping process and the ablation procedure, the physician puts the catheter tip in contact with tissue. At this specific point, the location of the catheter tip in the 3D space forms a 3D time series as time goes by.

In our study case, tens of positions at different locations are taken in the cardiac chamber for cardiac mapping. For each position, the corresponding fluoroscopy data is recorded. Moreover, the CF is recorded for reference as well.

At each position, the sequence of the catheter tip locations can be captured. There is an interesting phenomenon that the 3D data of some specific sequences of the catheter tip points, exactly form a 2D surface. The most important reason might be that the movement of the catheter tip is dominated by myocardium contraction when there is strong contact between the tissue and the catheter tip electrode. The observation gives some clue for the surface fitting idea. Figure 4-2 shows how all the points in a dataset fit a surface.

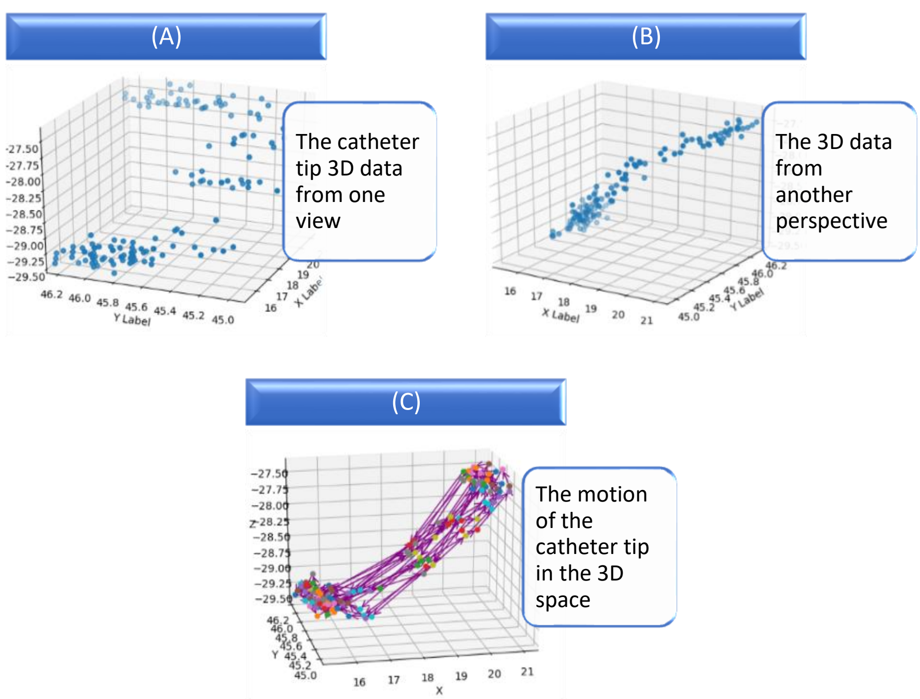

Figure 4-2 3D points fitting a plane. (A) The cloud of the 3D points fits a plane from one of the angles. (B) The view of 3D points fitting a plane from another angle (C) Moving motion of the tip, the direction showing with arrows.

4.2.3 Linear Plane Fitting and Quadratic Surface Fitting

As mentioned above, the 3D points can be fitted into a surface, the distance of these points to the fitting plane shows the density of the cloud, which means concentrated or sparse to the surface. This distance is related to the CF, which will be demonstrated in the section of the relation of 3D data and CF.

For the fitting surface, the points form a linear plane or quadratic surface? For simplicity, can the linear plane represent the motion of the catheter tip? In our study, a comprehensive dataset in a clinical study is applied to do the surface fitting. There are 21 datasets in total, Figure 4-3 below shows the surface fitting for one of the datasets using both linear and quadratic way. Figure 4-4 shows the comparison of average 3D distance to the fitting surface using all the 21 datasets.

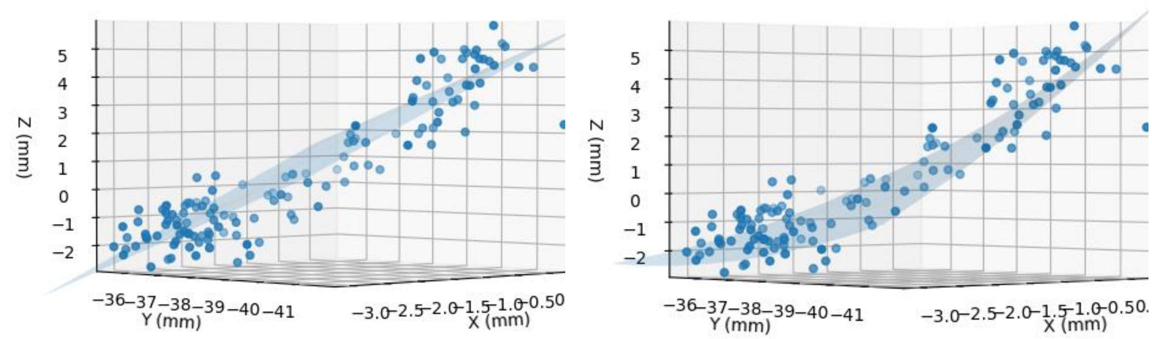

(A) (B)

Figure 4-3 Surface fitting of a 3D points dataset (A) Linear plane fitting. (B)Quadratic surface fitting

The ordinary least square is used for fitting a flat plane and quadratic surface in this case, which is minimizing the vertical offsets to fit a plane. Later more discussion will be made for vertical offset or perpendicular offsets. From the two different fittings, the average residual got by using the least square method is shown below. The correlation between these two results is almost one, which means there is no big difference in applying both ways for fitting. Figure 4-5 is the bar graph for the two different fittings. In this study, linear plane fitting is adopted for 3D data analysis.

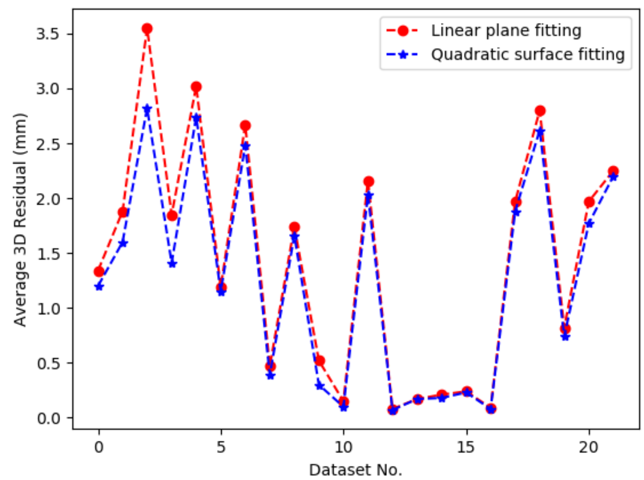

Figure 4-4 The comparison of surface fitting using linear plane fitting and quadratic surface fitting

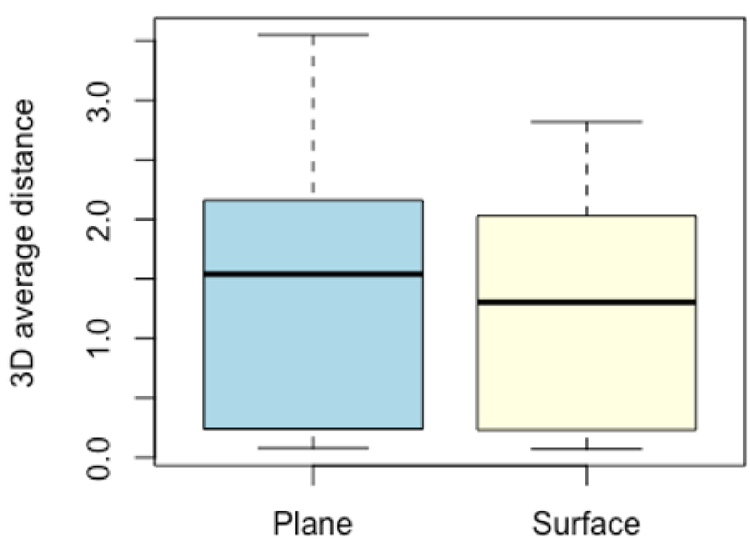

Figure 4-5 The bar graph of linear plane fitting and quadratic surface fitting for the same dataset in Figure 4-4. The mean value and the range of the 3D residual are very close.

4.2.4 Ordinary Least Squares and Total Least Squares

There are different ways to fit the plane, basically one is from the perspective of vertical offsets while the other one from perpendicular offsets. Ordinary least squares (OLS) is a type of linear least squares method for estimating the unknown parameters in a linear regression model. Geometrically, this is seen as the sum of the squared distances, parallel to the axis of the dependent variable. In our case, X and Y values are fixed, and the measured error is in Z-axis alone. For perpendicular offsets, it minimizes the orthogonal distances to the plane, which is called Total Least Squares (TLS).

(1) Ordinary Least Squares

Mathematically, this is a problem of approximately solving an overdetermined system of linear equations in our case, where the best approximation is defined as that minimizes the sum of squared differences between the data values and their corresponding modeled values.

A plane is generally described by a normal vector n = [a, b, c] ^{T} and a distance d. For point p = [x, y, z] ^{T} on the plane $\mathrm{np} + d = 0$, the plane can be written as: $\mathrm{ax} + \mathrm{by} + \mathrm{cz} + \mathrm{d} = 0$. As an overdetermined system, the goal is to find the coefficient β which fit the equations "best", in the sense of solving the minimization problem. X is a matrix of the points which contain the values from the X and Y axis, y is an array of the value of Z. Suppose we have m linear equation which means m points in the 3D space, the overdetermined system and how to get the coefficient can be expressed as follows:

$$\sum_{j=1}^{n} X_{ij}\beta_j = y_i \ (i = 1,2 \ldots, m) \tag{4.1}$$

$$\hat{\beta} = \arg\min S(\beta) \tag{4.2}$$

$$S(\beta) = \sum_{j=1}^{m} \left| y_i - \sum_{j=1}^{n} X_{ij}\beta_j \right|^2 = | y - X\beta |^2 \tag{4.3}$$

$$\hat{\beta} = \left(X^T X\right)^{-1} X^T y \tag{4.4}$$

Considering we are trying to fit the 3D points into a plane, As mentioned above, the average distance of these points to the fitting plane shows the density of the cloud, which means concentrated or sparse to the plane. From this perspective, OLS would not best represent this feature. Total least square below is what we adopted in this study.

(2) Total Least Squares

Total least squares is another way to fit the plane. Different with the OLS method, it checks from the prospective of the orthogonal direction. What is more, SVD and PCA are also able to process the 3D data for fitting a plane. Basically, the essential of all these three different ways are the same. It computes the orthogonal transform that decorrelates the variables and keeps the ones with the largest variance.

Suppose the dataset has been preprocessed to have zero mean, which the data matrix is X. The PCA viewpoint requires that one compute the eigenvalues and eigenvectors of the covariance matrix, which is the product XX^T, where $X$is the data matrix. Since the covariance matrix is symmetric, the matrix is diagonalizable, and the eigenvectors can be normalized such that they are orthonormal:

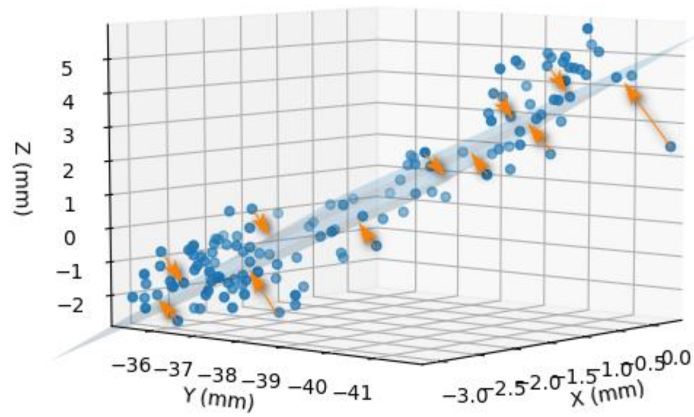

Figure 4-6 The average distance of all the points to the fitting plane, some blue arrows in the graph shows what is the distance from the point to the fitting plane.

$$XX^T = WDW^T \tag{4.5}$$

$$XX^T = (U\Sigma V^T)(U\Sigma V^T)^T \tag{4.6}$$

$$XX^T = (U\Sigma V^T)(V\Sigma^T U^T) \tag{4.7}$$

$$XX^T = (V\Sigma^2 U^T) \tag{4.8}$$

Now we can see the square roots of the eigenvalues of XX^T are the singular values of X. In fact, using the SVD to perform PCA is better numerically since formatting XX^Tmay cause loss of precision.

4.2.5 Plane Fitting Implementation

Previously ordinary least square and total least square are discussed. If the plane fitting method is certain, the distance of each point to the plane can be calculated. Navik system is used for part of the data collection in our study. The system is able to provide reliable 3D position but the X, Y values are more accurate the Z value, considering it provides the 3D location of the catheter tip from acquired 2D fluoroscopic images. In the implementation, the total least square is adopted for getting the perpendicular distance from the point to the plane. Moreover, to describe the concentration of the point cloud to the fitting plane, the average distance is computed. The perpendicular average distance reflects how concentrated of all the points to the fitting plane. If the distance is small, which means all the points are more densely gathered, otherwise, it shows the points are more scattered distributed in a 3D space. The general idea for getting a 3D catheter tip moving pattern is to perform a plane fitting based on perpendicular offsets at the beginning and further to get the average distance.

The average distance of all the points to the fitting plane shows the distribution of the points in the 3D space, which we expect stronger contact has a better plane fitting. Since the goal is getting the average distance of the 3D points to the fitting plane, how to calculate average 3D distance is the key issue, Suppose the 3D point is A (x0, y0, z0), and the projection is A'. The steps for the 3D distance computation is as follows:

(a) Get the function of the fitting plane. The plane is fitted to minimize the sum of the perpendicular distance of the points from the plane.

(b) Find the normal vector of the fitting plane. Normal vector is the vector perpendicular to the fitting plane, which is the direction for projection.

(c) Based on a single 3D point, get the value of the projection of the 3D point.

(d) Project all the points to get the distance.

(e) Get the average distance of all the points to the plane.

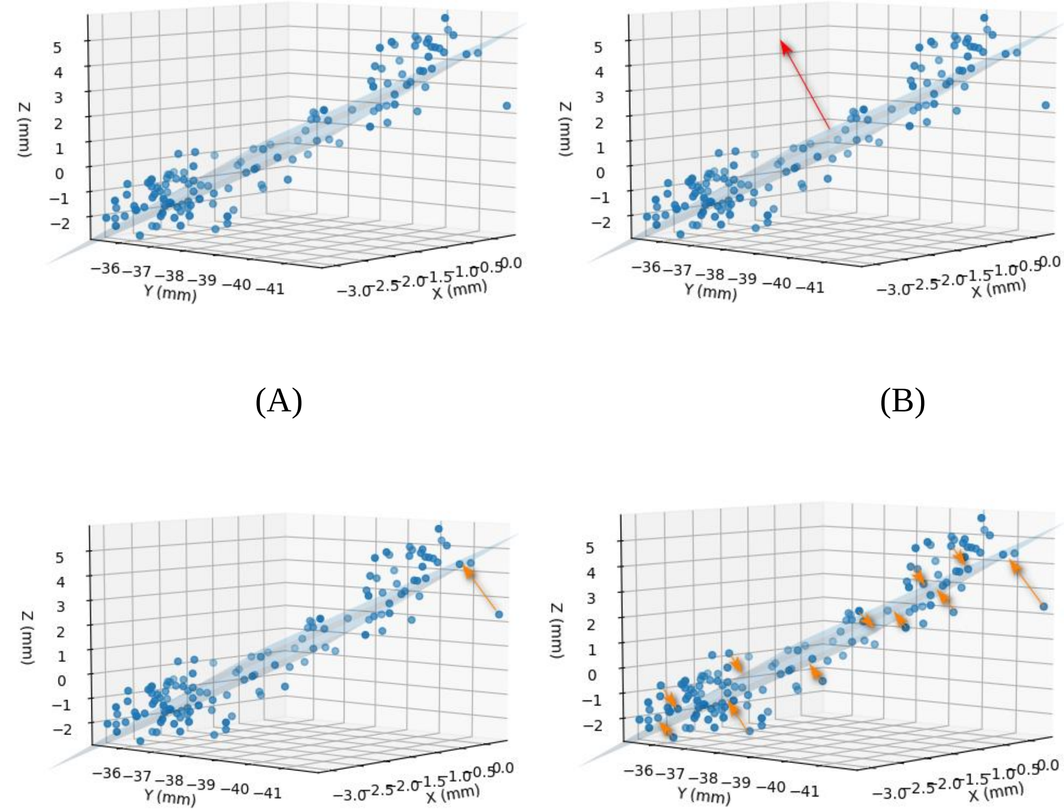

(A) (B)

(C) (D)

Figure 4-7 The process of getting the 3D average distance, the first graph completes a plane fitting, the second one shows the normal vector of the plane, which is perpendicular to the fitting plane. When the points project to the plane to get the distance, it follows the direction of the normal vector which is perpendicular. The third graph shows one-point projecting to the plane to get the point to plane distance. The last graph shows different points projecting to the plane, finally, the average distance can be obtained.

4.2.6 The Relation of 3D Data and CF

If there is strong contact between the electrode and tissue, the primary factor affecting the tip movement should be myocardium contraction, otherwise, there might other factors dominating tip movement. For instance, blood circulation, breathing and so on. Thus, it is easier for all the points forming a plane when there is a strong contact. The figure below shows a comparison of two datasets with different CF level, one is in strong contact while the other one in weak contact.

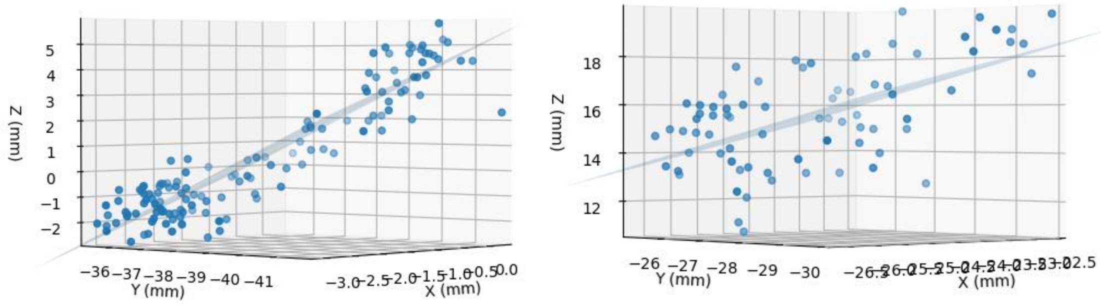

(A) (B)

Figure 4-8 A comparison of two datasets with strong and weak CF respectively

(1) The relationship between CF and the 3D average distance

In one of the studies, the 3D data and the corresponding CF value were collected. The plan was to collect the data at ten different positions with strong, normal, weak contact which should be 30 datasets in total, 2 datasets are skipped during the operation, so there are 28 datasets which include 56 DICOM video from the different positions. There are 7 datasets missing the catheter tip in the LAO view within the range of the fluoroscopy, which made it impossible to generate the 3D location, so eventually, 21 datasets are used for analysis.

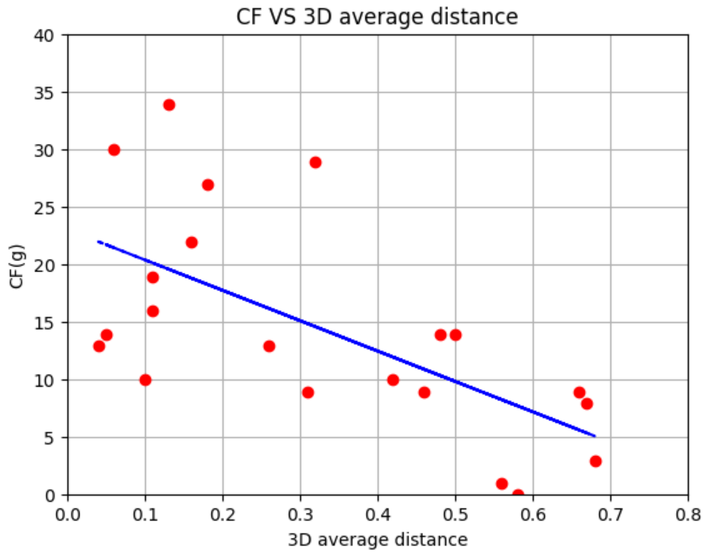

Figure 4-9 CF VS 3D average distance (perpendicular offsets)

Figure 4-9 shows the relationship between CF and 3D average distance. Linear regression is applied for analysis, it can be observed that the CF is sort of inversely related to the value of the 3D average distance. The R-squared value is 0.32. Suppose the CF prediction can be obtained using the points projecting to the line to get a corresponding value, and the measured CF is provided for these 21 datasets as a reference, these two datasets can be taken to make a comparison. Figure 4-10 shows a comparison, for our evaluating system, the CF value only needs to be set into four ranges instead of a specific value. Figure 4-11 shows the measured CF value and the prediction CF value after normalizing the CF value into four ranges which are “strong”, “good”, “medium” and “weak”. In the graph, these are represented using the number from one to four.

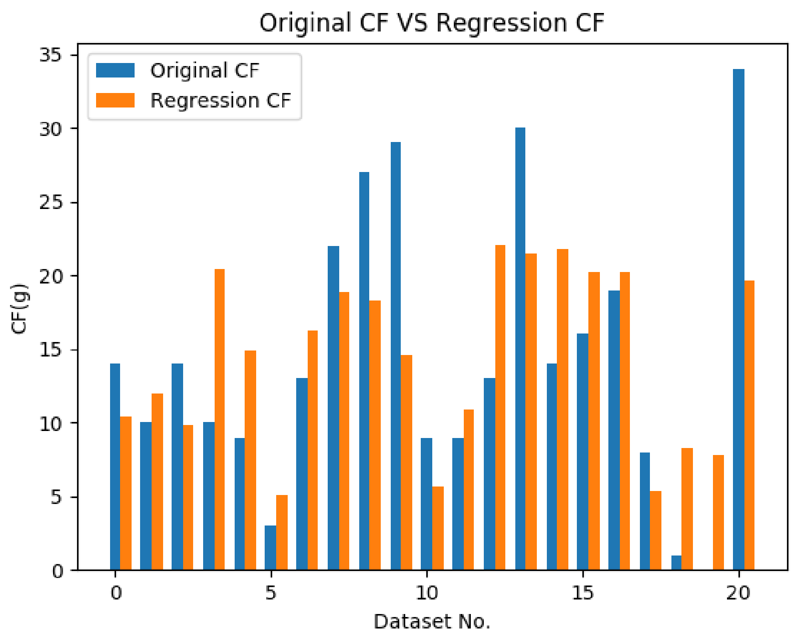

Figure 4-10 The comparison of the regression CF and original CF after TLS processing.

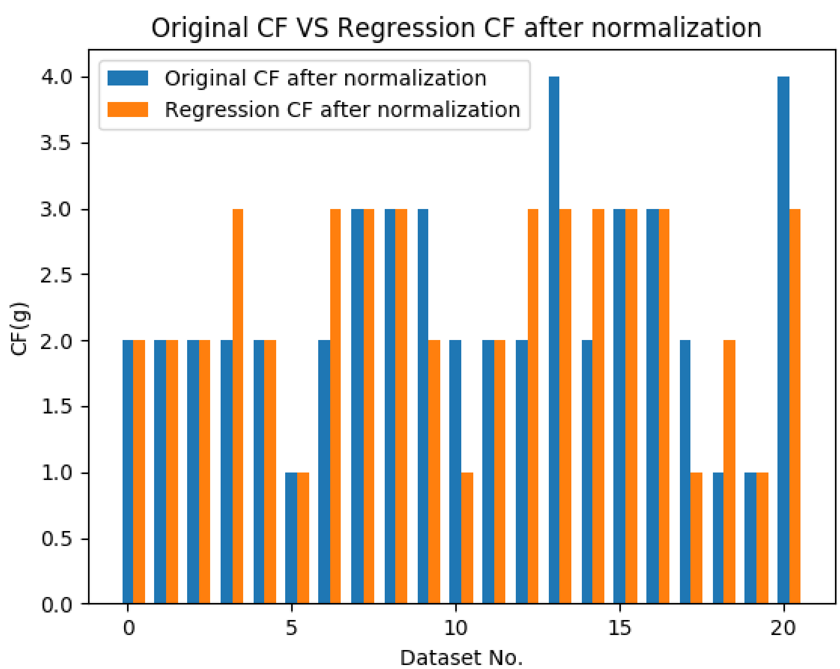

Figure 4-11 The comparison of the normalized regression CF and original CF after normalization considering we are setting the CF range into weak, medium, good and strong. CF level is lowest at 1, highest at 4 in the figure above.

(2) Bootstrapping for generating data

In the clinical study, so far, the data collected is very small datasets. Bootstrapping is used for regenerating some sample data for the analysis. The basic way is sampling from the original dataset with replacement. From the graphs, we can see it is very similar to the distribution for X, Y, Z values.

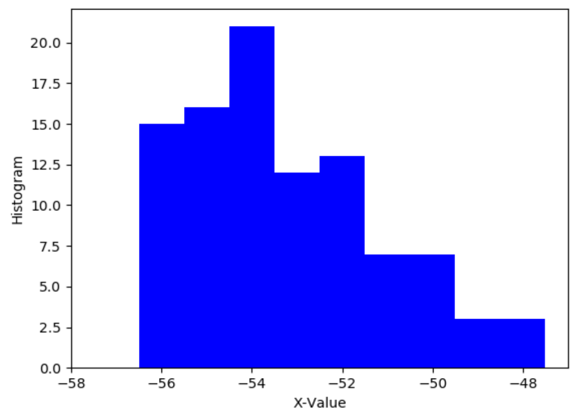

(A)

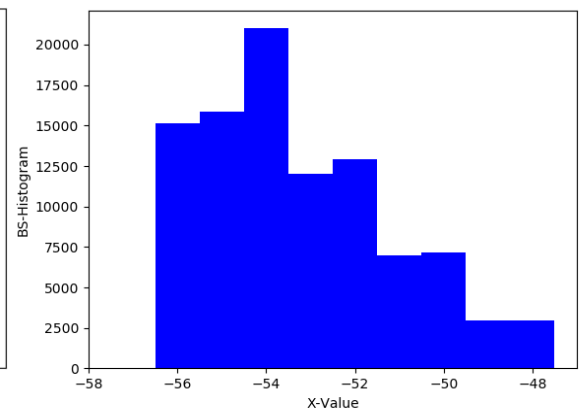

(B)

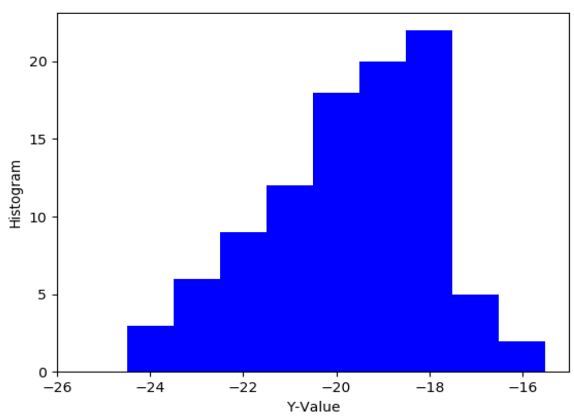

(C)

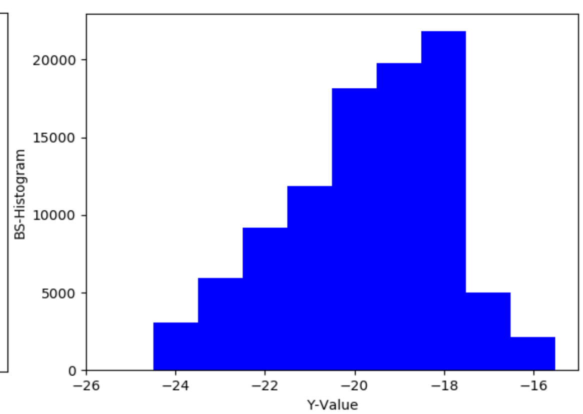

(D)

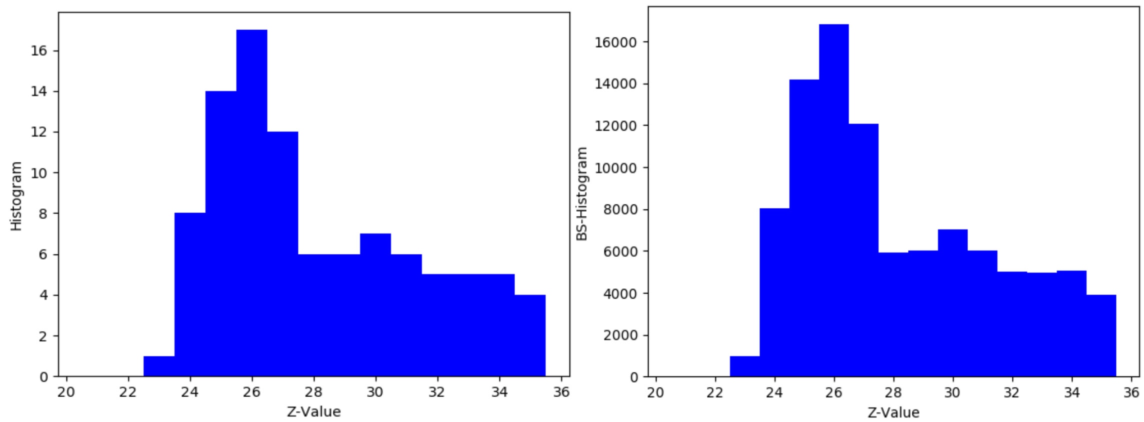

(E) (F)

Figure 4-12 The original dataset and the bootstrapping data histogram (X, Y, Z) Figure (A) is the original data histogram for the X data from 3D space, figure(B) is the resampled data histogram for X data. Figure(C) (D) and (E) (F) are for Y data and Z data respectively.

(3) Confidence Interval analysis

Since more data is generated using bootstrapping, a confidence interval can be computed using the data. In our case, taking the 3D residual for instance. In the study, we pick up one 3D dataset with a CF value as original sample data. (The data has 97 3D points). Later generate more sample data using the original data using bootstrapping sampling. The basic process is as follows:

- Generate 10000 sample dataset using bootstrapping. Thus, we have 10000 samples of 3D points with a certain level of CF.
- Compute residual: For each sample 3D points, calculate the residual.
- Get the residual statistics.
- Compute the 95% Confidence Interval

Confidence Interval	80%	85%	90%	95%	99%	99.5%	99.9%
Z	1.282	1.440	1.645	1.960	2.576	2.807	3.291

Table 4-1 The confidence Interval and Z value

The confidence interval is computed as: X ± Z*s/Sqrt(n), in our case, the confidence interval is 203.9 ± 0.58.

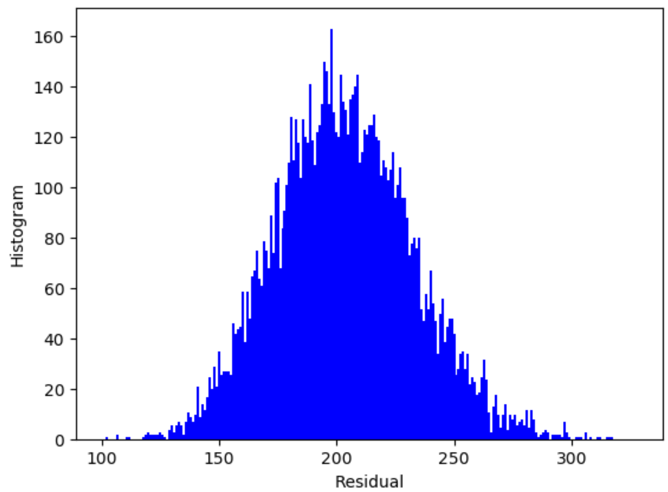

Figure 4-13 bootstrapping data histogram of the residual

4.3 Two-Dimensional Data Analysis

4.3.1 Catheter Tip 2D Data Description

There are two typical fluoroscopic views which are the AP view and the Lateral view, 3D data can be generated using the back-projection algorithm. Based on these two views, 2D data is available from two different perspectives, but considering the tilting angle of the cloud of the 3D points may affect the distribution, the 2D data applied in our study comes from the projection data of the 3D points. Plane fitting is mentioned in the previous section, the projection of the 3D points on the plane includes some significant information. Based on the projected 2D data, the points distribution is long and narrow with higher CF while with a smaller CF goes to the other way, Principal component analysis (PCA) is a good way to describe it. As for PCA, the purpose is not for dimension reduction but to get the ratio of the primary component and the secondary primary component to describe the shape. Figure 4-14 shows a 3D points projection on a plane and how a 2D projection to the plane looks like.

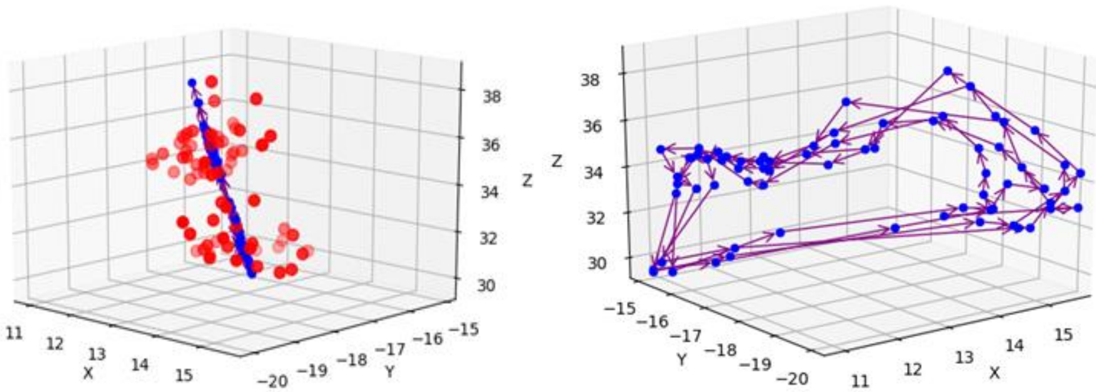

(A) (B)

Figure 4-14 A dataset showing the 3D data and 2D projection

4.3.2 Analysis Methods

The motivation for applying the 2D data is because the shape of the points distribution seems related to CF in the study. The eigenvectors of the 2D points can be used to get the ratio of the long axis and short axis. The primary component and the secondary primary component of the 2D data based on projection can be got to describe the shape (considering the points distribution may like an eclipse). Except for PCA, actually, eigenvectors calculation or singular-value decomposition (SVD) can also decide the ratio of the long axis and the short axis of the 2D points. Suppose the projected 2D data is provided, the following steps can be applied for calculating the ratio between the long axis and the short axis.

(a) Processing the data, form a matrix X which composed by m*n

(b) Initialization get the mean value of each row and subtracted by each element

(c) Get the covariance matrix $C = XX^T/(m-1)$

(d) Arrange the eigenvectors according to the size of the eigenvalues, get the direction for the long axis and short axis.

(e) Based on the direction of the long axis and short axis, the value of all the points, get the ratio of the long axis and the short axis.

4.3.3 The Relation of 2D Data and CF

The shape of the 2D points distribution reveals some information related to CF. Based on observation, the points distribution is long and narrow when CF is strong. The following graphs show a comparison of the 2D axis with different CF levels.

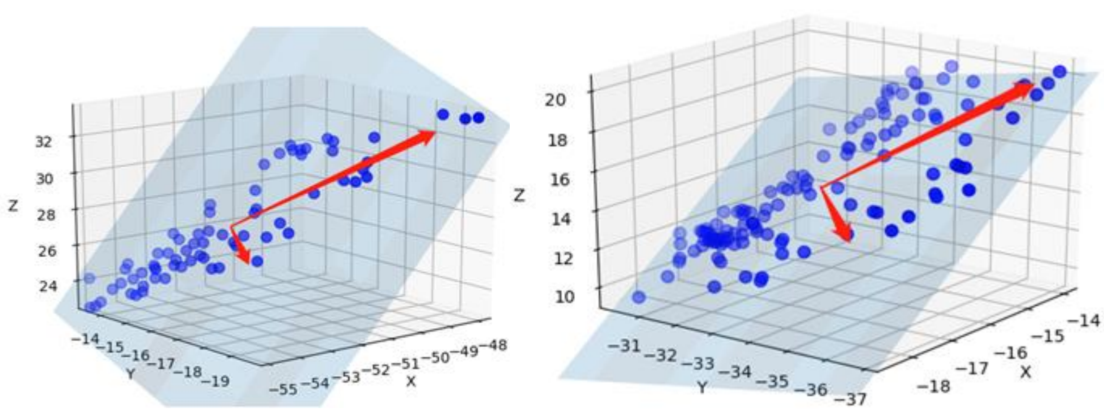

(A) (B)

Figure 4-15 2D axis comparison with strong and weak CF respectively

Here I applied the 2D data from the projected view for analyzing using PCA. Linear regression is applied for analysis, the R-squared value is 0.32. Following the steps mentioned above, the primary component and secondary primary component can be computed for all the points in the dataset, there are 21 datasets in total, the graph below shows the relationship between the 2D ratio and CF.

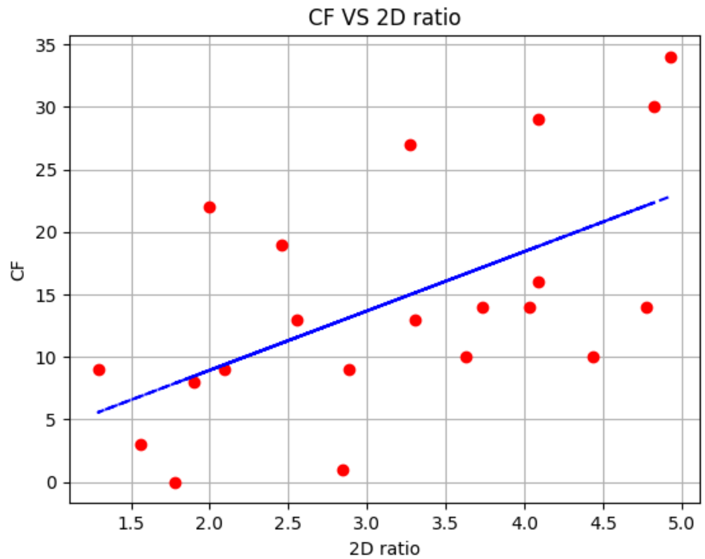

Figure 4-16 CF VS 2D ratio.

Similar to the process for the 3D average distance, Figure 4-17 show the comparison of the original CF and regression CF using the 2D ratio as parameter. Figure 4-18 shows the difference after normalizing the CF into four ranges.

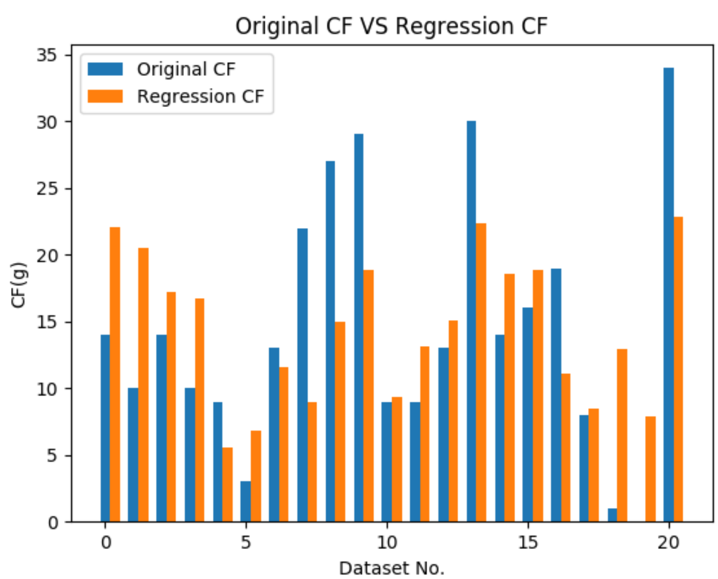

Figure 4-17 The comparison of the regression CF and original CF after TLS processing using the feature of 2D ratio.

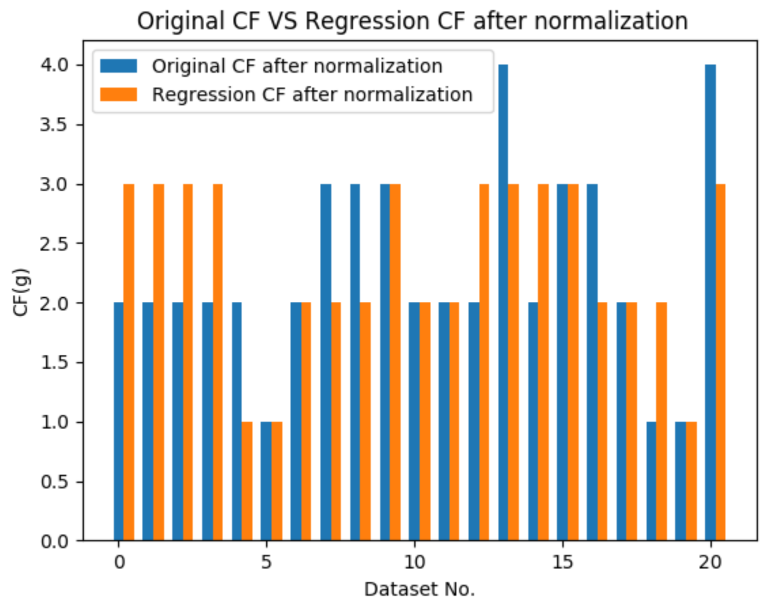

Figure 4-18 The comparison of the normalized regression CF and original CF after normalization using the feature of 2D ratio. Considering we are setting the CF range into weak, medium, good and strong. CF level is lowest at 1, highest at 4 in the figure above.

Form the comparison we can see that the 2D ratio and CF has a positive correlation. The value of the regression CF after normalization and the true value are the same for most of the pairs.

4.4 One Dimensional Data Analysis

4.4.1 Catheter Tip 1D Data Description

The position of the catheter tip, if depicted in a 3D space, includes the X, Y, Z coordinates which represent the spatial information. Within a certain time, the moving track of the catheter tip can form a time series, which is a series of data point indexed in time order. There is specific physical meaning for each dimension in the 3D space. Patient lays on the table between the X-ray source and the fluoroscopy detector, Thus, X and Y are the components perpendicular to the projector and Z represents the distance from the catheter tip and the X-ray source. The time series is a sequence measurement over time. Each of the X, Y, Z components can be extracted to be displayed in a sequence followed by time order, which is the 1D time series in this section. The figure below shows a dataset with the X, Y, Z 1D time series.

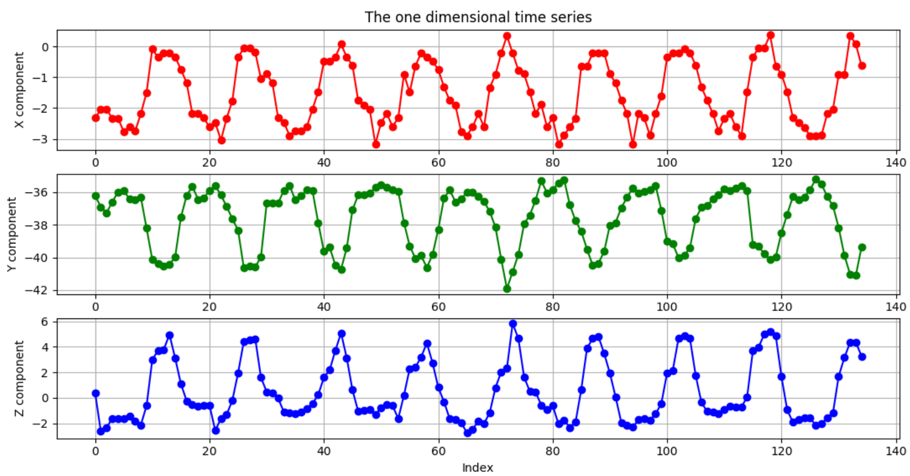

Figure 4-19 The time series from X, Y, Z directions of a 3D catheter tip location, collected on September 18th, 2012

The 1D time series can be cut by using the R wave or other related information to get short time series in each cardiac cycle. The data from X, Y, Z components are displayed in a sequence followed by time order. A trend of the one-dimensional moving pattern can be observed. If separate the time series by cardiac cycles, the R waves can be applied as boundaries. Thus, the catheter tip moving track can be cut into shorter time series. The figure below shows the separated short time series.

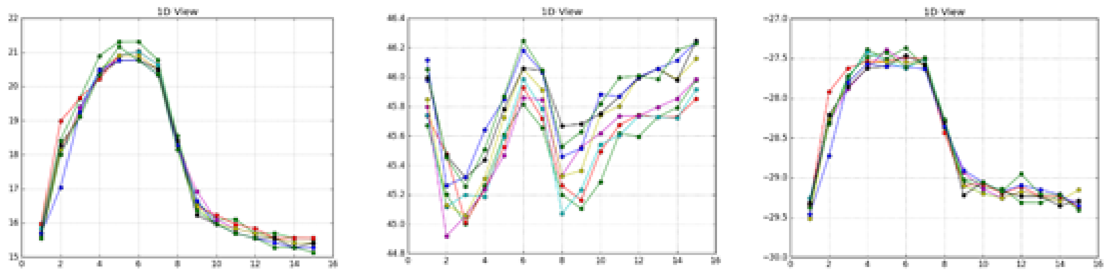

(A) (B) (C)

Figure 4-20 The figure(A)(B)(C) above shows the time series from X, Y, Z components of one dataset separated by the cardiac cycles

4.4.2 Analysis Methods

The similarity of the short time series from the X, Y, Z components is related to the stability of the catheter-tissue contact during the catheter ablation. The observation of the clinical data shows strong tissue-tip contact may bring a more regular catheter tip moving pattern. The short time series could even be overlapped for some extreme cases. In the study, we assume that it is more similar for the short time series with a stronger electrode-tissue contact.

Thus, quantify the similarity of the short time series is the problem needs to be solved. Suppose the length of the time series are the same, it is easy to build to model to measure the distance. Unfortunately, even though the cardiac cycle duration is sort of stable, the length of the short time series is similar but not always the same. Dynamic Time Warping (DTW) is an effective way to measure the difference between time series, it works even though the length of the two time series vary.

DTW is firstly proposed by Berndt and Clifford (1994) [80]. Start by constructing $n \times m$ matrix. A warping path w is a contiguous set of matrix elements which defines a mapping between x and y that satisfies the following condition. The similarity computation using DTW gets a certain value, which can also be called cost. Suppose there are two known time series x and y with length M and N respectively:

T1 = [45.0759, 47.8144, 47.4028, 45.493, 43.4521, 43.932, 44.4311, 44.3998, 43.5171]

T2 = [44.0864, 45.9625, 44.4701, 41.5546, 40.5767, 43.5365, 44.5413, 44.2434, 44.9174, 44.7689]

Two time series T1, T2 are from two consecutive cardiac cycles, the data is extracted from the 3D catheter tip position using the X dimension data. For T1, it has 9 points in one cardiac cycle while the other has 10 points in another cardiac cycle. The following steps are applied for calculating the cost.

(a) Building a two-dimensional matrix to get the distances using two time series T1 and T2. The distance is defined using Euclidean distance. The distance can be treated as cost.

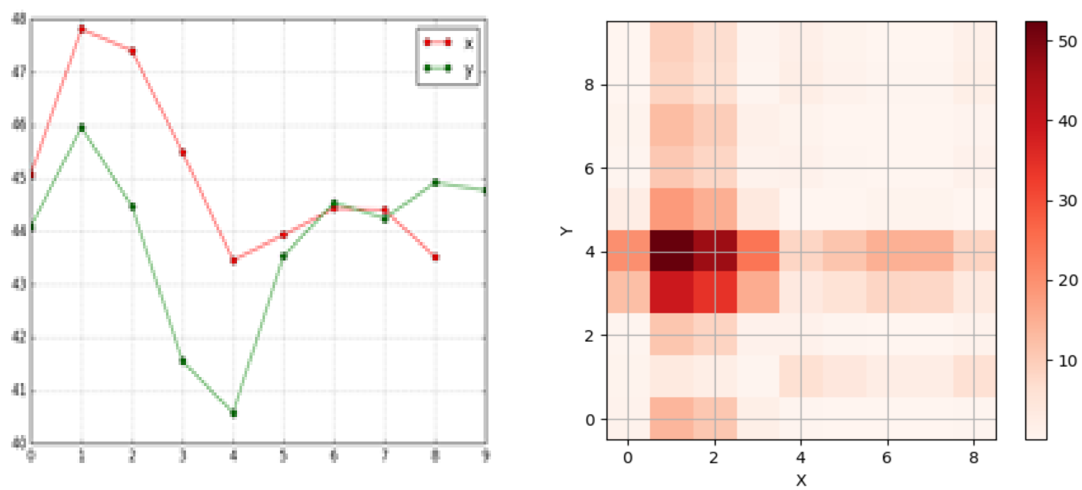

(A) (B)

Figure 4-21 (A)Two short time series from two consecutive cardiac cycles which extracted from one dataset. (B) 2D matrix for T1 and T2, each lattice in the matrix means the distance of the corresponding element from T1 and T2. The darkness of the lattice means the distance value, the darker, the distance is bigger.

(b) Building up the accumulated cost matrix.

The calculation starts from the point of (0, 0) , keep computing until goes to the end point (M, N). What is more, the path cannot be reversed, there are three directions: go towards to the right; go towards upwards; go towards the diagonal direction. Keep doing that until reaching the ending point (M, N). Finally, the accumulated cost can be obtained in this matrix.

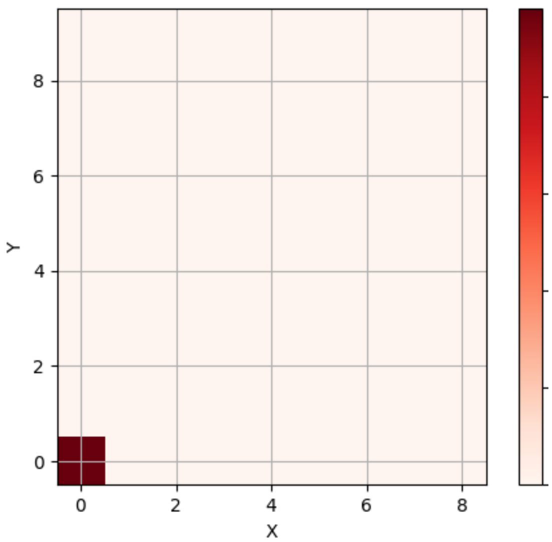

(A)

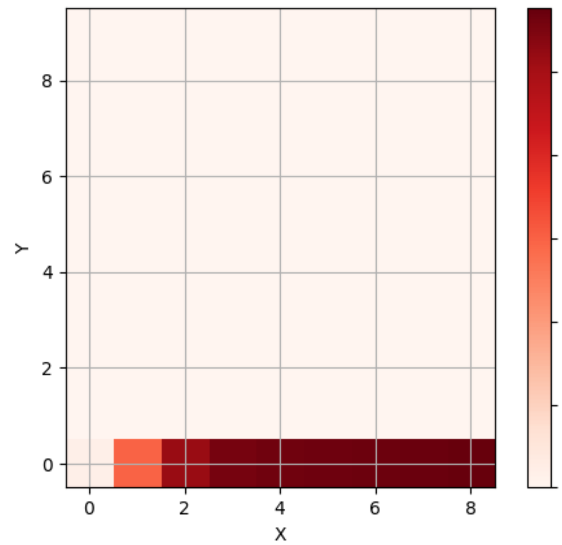

(B)

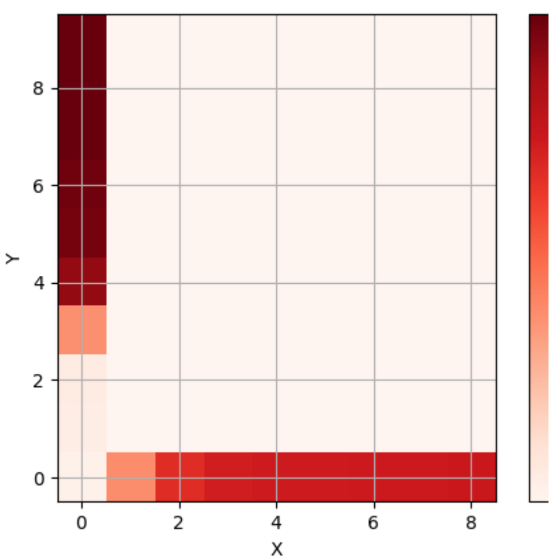

(C)

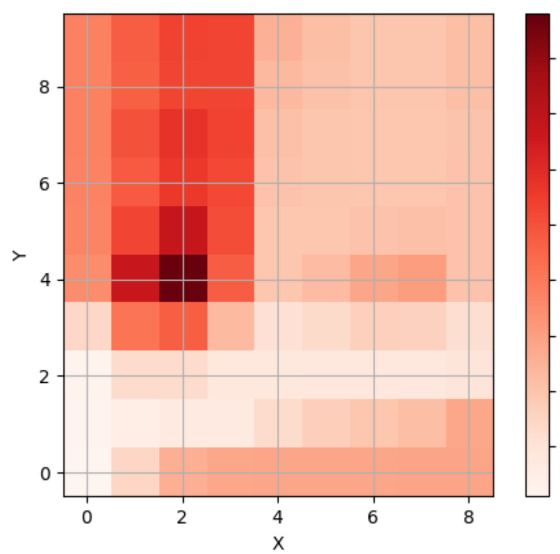

(D)

Figure 4-22 The process of building up the accumulated cost matrix. (A)Start point located at (0, 0). (B)Go forward towards the right direction. (C)Go forward towards the right and upper direction. (D) Go forward towards the right, upper and diagonal directions and obtain the accumulated cost matrix [80]..

(c) Backtracking and finding the optimal warp path.

Backtracking to get the optimum path. After the work done in step 2, the accumulated cost matrix has been built and now need to track the path with the minimum cost. Backtracking procedure basically is calculating from the end point to the starting point to find the path with a goal of minimizing the cost.

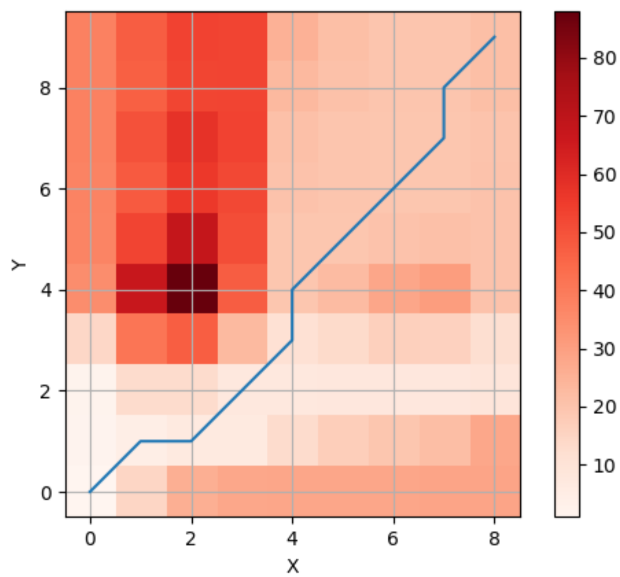

Figure 4-23 The optimum warping path which minimizes the sum of distance (DTW distance) along the path

4.4.3 The Relation of 1D Data and Catheter CF

(1) Selection of X, Y, Z components for 1D cost.

The time series similarity computation is based on one-dimensional data, since X, Y, Z components are applied for computation, checking the correlation among them could be the first thing need to be explored. But actually, for the 1D time series comparison, what we can see is that the periodic motion pattern most clearly in X, one reason is that the poor image quality in the second view of each pair may affect the accuracy. The second view(s) are taken from laterally (from the patient's side) and involve a thicker cross-section of the patient's torso. These lateral views always seem to be much poorer than the AP (patient front to back) view sometimes. Considering these factors, X component is taken for the 1D cost.

(2) The relation between time series similarity and CF

The following figure shows the relation of the time series similarity which is the cost and the CF. The similarity is computed using the X component. Basically, we can see the contact force is stronger, and the cost is lower.

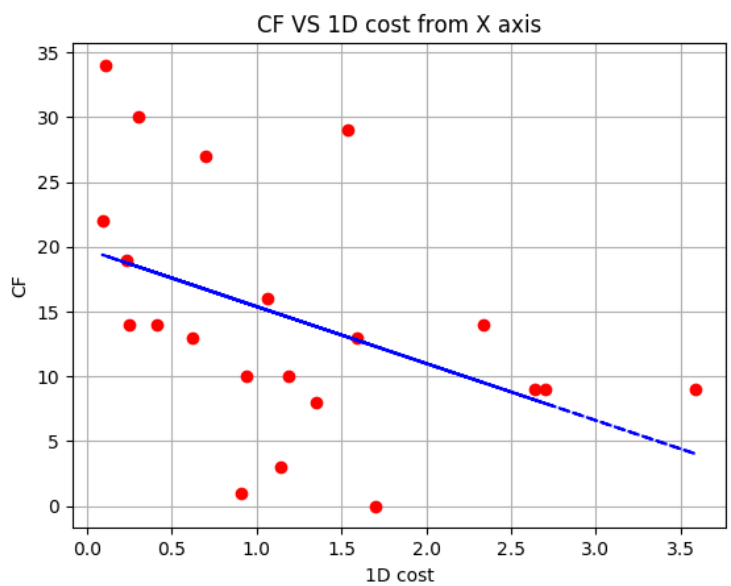

Figure 4-24 CF VS 1D Cost

Similar to the process for the 3D and 2D parameters, Figure 4-25 show the comparison of the original CF and regression CF using the 1D cost as parameter. Linear regression is applied for analysis, the R-squared value is 0.22, the association is kind of weak. Figure 4-26 shows the difference after normalizing the CF into four ranges.

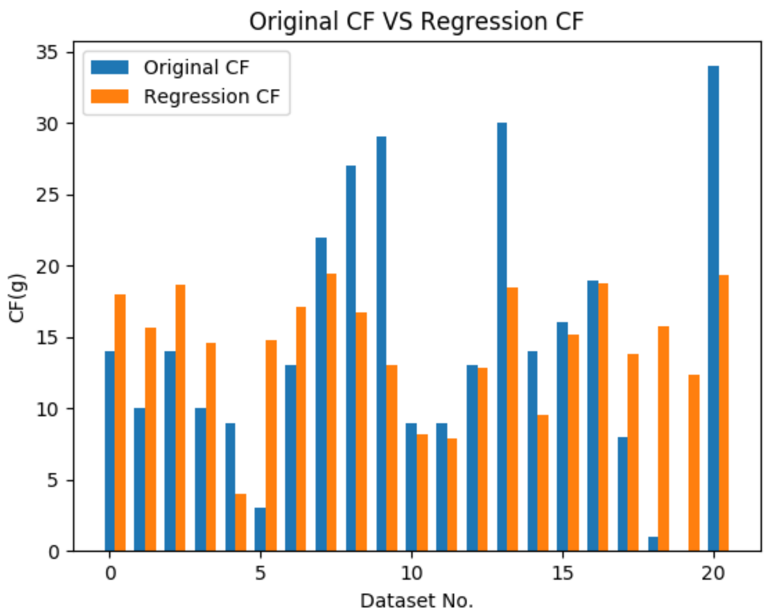

Figure 4-25 The comparison of the regression CF and original CF after TLS processing using the feature of 1D cost.

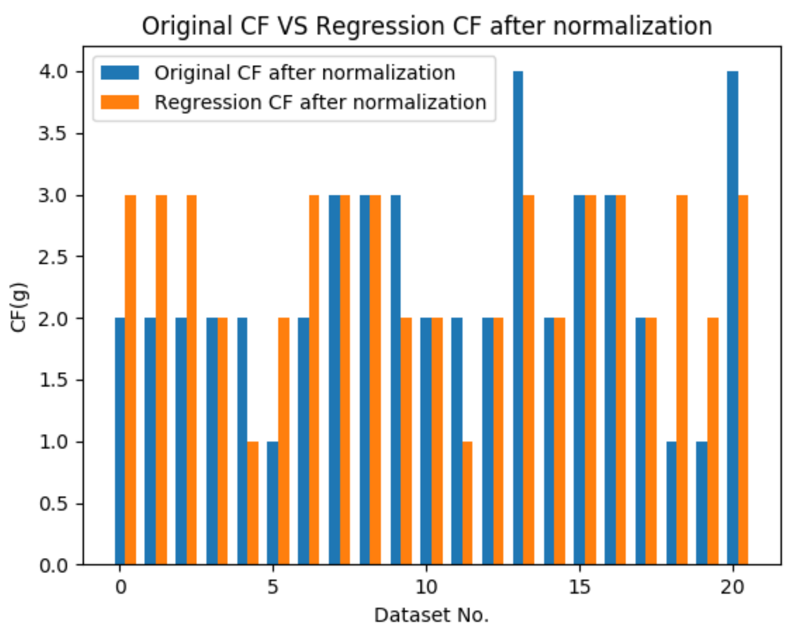

Figure 4-26 The comparison of the normalized regression CF and original CF after normalization using the feature of 1D cost. considering we are setting the CF range into weak, medium, good and strong. CF level is lowest at 1, highest at 4 in the figure above.

4.5 Correlation between the features

The relationship between the CF and three different features have been discussed in the previous sections. Normally when we have a dataset, probably there is a plethora of features in the dataset. All of the features we find in the dataset might not be useful in building a machine learning model to make the necessary prediction. Using some of the features might even make the predictions worse. Thus, feature selection plays a huge role in building a machine learning model, this section we will look into if there is any correlation between those three features.

Features with high correlation are more linearly dependent and hence have almost the same effect on the dependent variable. So, when two features have high correlation, we can drop one of the two features, otherwise, we should keep it.

When evaluating the correlation between all the features, a correlation matrix can be built, the correlation of each feature with itself, which is always 1. The other lattices show the corresponding relationship between different features. The graph below shows the correlation matrix of the three features selected in the research; it has the red diagonal from the upper left to the lower right. Other than the diagonal, the rest of the squares show correlation between different features, what we can see here is “3D distance” and “2D ratio” is not really related, but “3D distance” and “1D cost” is kind of related but very week, it is much less than 0.9, which can be ignored.

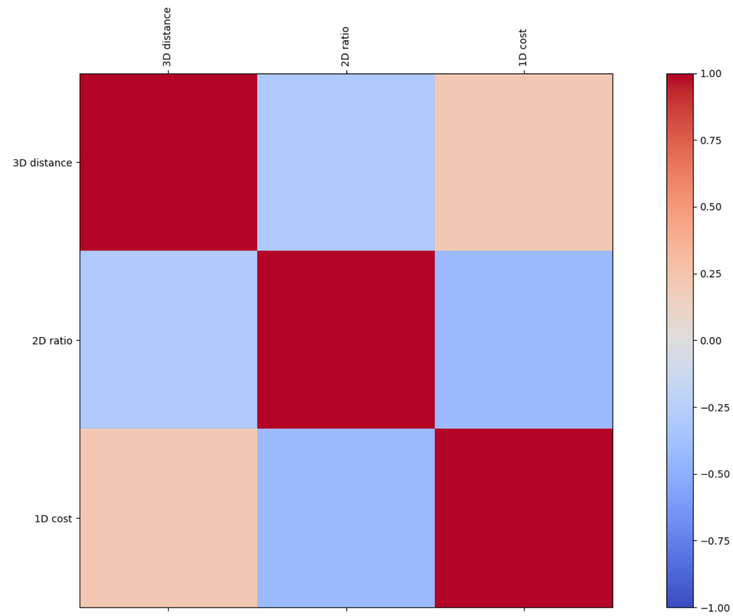

Figure 4-27 Correlation heatmap for the Dataset

So based on the correlation matrix, it can be concluded that all three features are necessary and are not supposed to eliminated. If there are more features applied for CF evaluation in the future research, a correlation matrix can still be built to analyze the process of the feature selection.

4.6 The CF prediction

In the previous sections, the features extracted from the moving pattern of the catheter tip are used to analyze the relationship between the CF and the corresponding feature such as 3D average distance to the fitting plane, 2D ratio, and 1D cost. From the results analysis, we can see it is inversely proportional between the 3D average distance and the CF to some extent, in the meanwhile, there is somewhat proportional relation between 2D ratio and 1D cost to CF. Since these features are demonstrated to valuable for evaluating CF, the further question is that if we can use the motion of the catheter tip within a certain time window to predict CF.

4.6.1 The range of the features from the historical data

A certain parameter such as 3D average distance is related to the CF when CF varies, but the range of the 3D average distance is not known yet. Considering the variability among different patients, there is clinical data provided by APN Health to get the range for each parameter used in the research. The table as follows shows 24 datasets collected from 8 patients, there is at least one pair of breathing & apneic data for each patient, some patients have more than one pairs.

Patient No.	Data collected position	Collected datasets	Heartbeat
1	LSPV	2	Regular
2	LSPV	2	Regular
3	Regular MPV	2	Irregular
4	LSPV	2	Regular
5	LIPV	2	Irregular
6	LSPV	2	Regular
7	LIPV, regular SPV	8	Irregular
8	LIPV, LSPV	4	Irregular

Table 4-2 the data collected from 8 patients.

By using the 3D location data of the catheter tip from the 24 datasets above, the average 3D distance, 2D ratio, and 1D cost are calculated to get the range of these parameters for evaluating CF. More data collected, the database would be more concrete, based on our current data, the range of the history data and range of test data is very close.

For instance, from the figure below we can see the range of 3D average distance are very similar between the historical data and the test data.

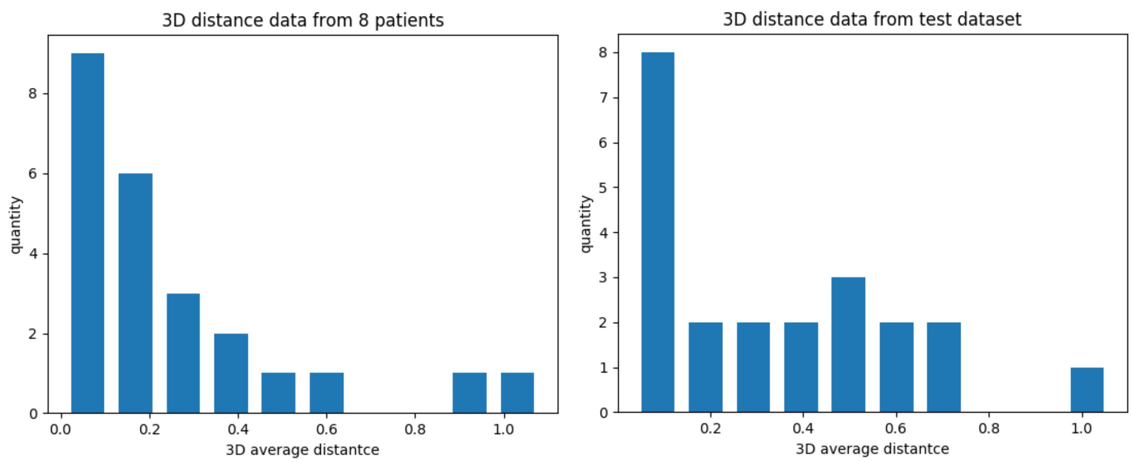

(A) (B)

Figure 4-28 The comparison of the range of 3D average distances (A) 3D average distance to the fitting plane from history data. (B)3D average distance from test dataset.

4.6.2 Setting the range for the test data

The output of the CF prediction is not consecutive values, instead, the CF predicting results are separated into four ranges, which are weak, medium, good, and strong. If the CF is weak, which means it needs to be enhanced, medium is a good electrode-tissue contact level, but not perfect, the range of good CF is the best fit during catheter ablation. Strong CF might cause perforation. Thus, CF located in this range reminds the physician paying attention to the contact strength. Previous studies [23,26] suggested an optimal CF range to form proper lesion size during the radiofrequency ablation procedure, considering the four ranges set for analysis, how to identify the CF range is shown as follows:

Weak: $\{f \mid 0 < f \leq 5\}$

Medium: $\{f \mid 5 < f \leq 10\}$

Good: $\{f \mid 10 < f \leq 30\}$

Strong: $\{f \mid f > 30\}$

Unlike the feature analysis part, the CF prediction involves all the three different features to decide the output based on a decision tree. The inputs are consecutive values. Thus, it is necessary to set the range for each input to get the discrete input. Based on the current data collected, the 3D average distance and 2D ratio are distributed into three pieces evenly, the 1D cost provide the information of time series similarity, in this research it is separated into two parts, which means similar or dissimilar.

Based on the history data, the range of the 3D average distance can be set as:

Small: $\{x \mid 0 < x \leq 0.25\}$

Medium: $\{x \mid 0.25 < x \leq 0.5\}$

Big: $\{x \mid x > 0.5\}$

The range of the 2D ratio can be set as:

Small: $\{y \mid 0 < y \leq 2\}$

Medium: $\{y \mid 2 < y \leq 4\}$

Big: $\{y \mid y > 4\}$

The range of 1D cost can be set as:

Similar: $\{z \mid z \leq 0.8\}$

Dissimilar: $\{z \mid z > 0.8\}$

To fit the inputs for the decision tree, the dataset collected from a comprehensive study with CF as reference following range setting using the history data.

4.6.3 An example for CF prediction based on multi-class decision tree

In a clinical study case, there are 21 datasets collected as follows, as the range setting has been mentioned above, the numeric values of different parameters are classified into ranges. Each one has the range of the attributes and the corresponding CF value as reference.

Dataset	3D	2D ratio	1D cost	CF
1	medium	big	similar	good
2	medium	big	dissimilar	good
3	big	medium	similar	good
4	small	medium	dissimilar	good
5	medium	small	dissimilar	medium
6	big	small	dissimilar	weak
7	medium	medium	similar	good
8	small	medium	similar	good
9	small	medium	similar	good
10	medium	big	dissimilar	good
11	big	medium	dissimilar	medium
12	medium	medium	dissimilar	medium
13	small	medium	dissimilar	good
14	small	big	similar	strong
15	small	big	dissimilar	good
16	small	big	dissimilar	good
17	small	medium	similar	good
18	small	small	dissimilar	medium
19	medium	medium	dissimilar	weak
20	big	medium	dissimilar	weak
21	small	big	similar	strong

Table 4-3 A comprehensive dataset including the features extracted from the moving pattern of the catheter tip and the corresponding CF.

Since the output is set into four different labels, thus, four datasets from the above cover the four different labels are taken as test data, all the rest are used as training data.

Dataset	**3D**	**2D ratio**	**1D cost**	**CF**
21	small	big	similar	Strong
1	medium	big	similar	Good
5	medium	small	dissimilar	Medium
20	big	medium	dissimilar	Weak

Table 4-4 The test data randomly extracted from the dataset above mentioned in table 4.1

Based on the dataset, the following graph shows the binary decisions for combing to get the multiclass classification tree. The amount of the decision tree is six since there are four outputs, the output is strong, good, medium and weak, thus, the combination includes “strong-good”, “strong-medium”, “strong-weak”, “good-medium”, “good-weak”, “medium-weak”.

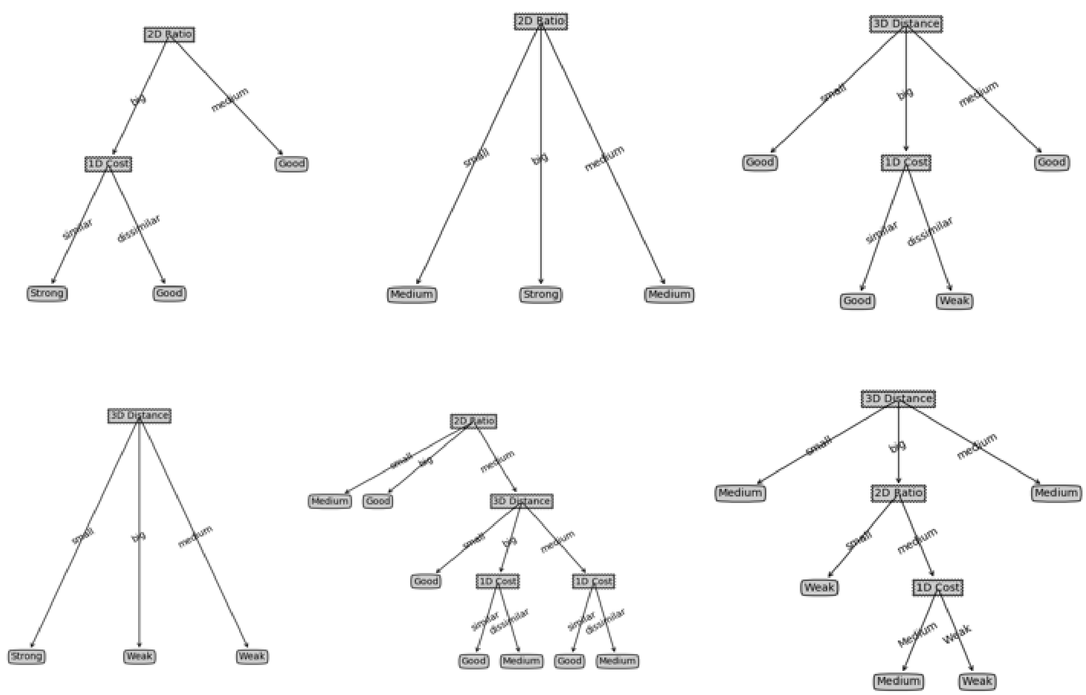

Figure 4-29 The decision trees combing to get the multiclass classification tree. There are six decision trees which represent the combination of “strong-good”, “strong-medium”, “strong-weak”, “good-medium”, “good-weak”, “medium-weak”

After all the binary decision trees are built, the multiclass can be classified using the test data in Table 4-4. Each tree run the data and get one output. The process is just like voting, the CF level is determined by the output which gets the highest votes. For instance, one of the test datasets is as following in the table, after the inputs go through each of the decision tree, the output “strong” gets the highest votes, which means that is the final output.

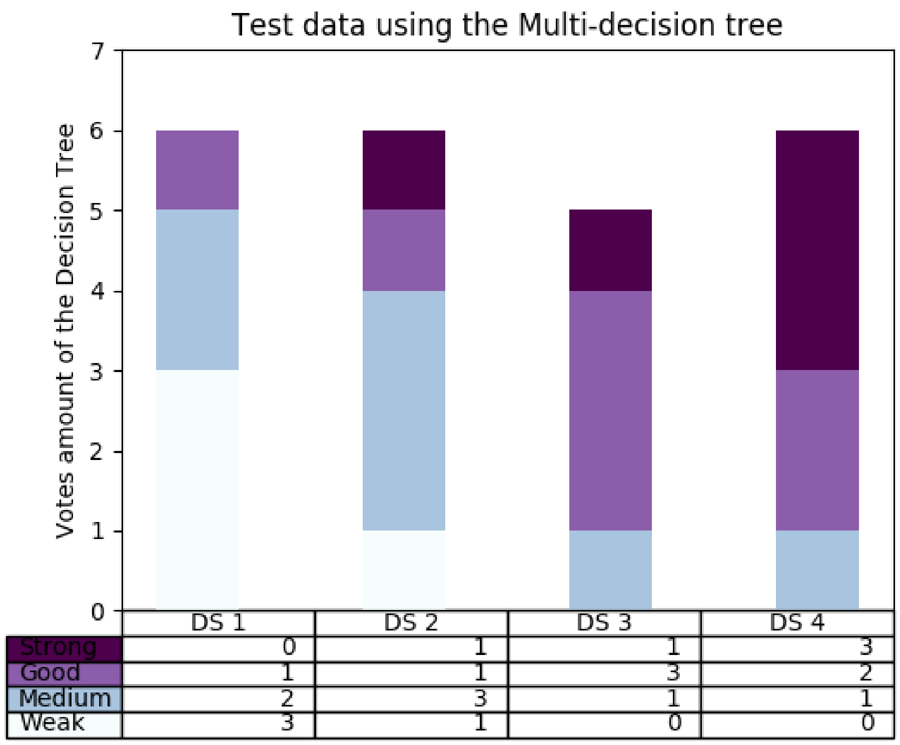

Figure 4-30 Multi-decision tree voting for the four test data sets

Test Dataset	3D	2D ratio	1D cost	CF	Predicted CF
21	small	big	similar	Strong	Strong
1	medium	big	similar	Good	Good
5	medium	small	dissimilar	Medium	Medium
20	big	medium	dissimilar	Weak	Weak

Table 4-5 Comparison of the CF and predicted CF using the test data

The test data is selected from the clinical study mentioned in table 4-4. From the measured CF, four datasets with different measured CF are used for test data, all the rest is used as training data. From the comparison of the measured CF and predicted CF we can see it is very accurate using the collected features extracted from the moving pattern of the catheter tip. After more training datasets are added, the decision tree can be updated. From the datasets we used for analysis, some of the binary decision tree does not have lots of branches since the related training data is not sufficient, since more data taken for training, it would be more compatible for different chamber locations and different patients.

4.6.4 Cross Validation for CF prediction

Cross Validation can be used to assess the predictive performance of the models and to judge how they perform outside the sample to a new data set. The motivation of using cross validation techniques in our research is that when we fit a model, we are fitting it to a training dataset. Without cross validation we only have information on how the model performs to the in-sample data. Ideally, it would be good to see how the model performs when we have a new data in terms of accuracy of its predictions. In science, theories are judged by its predictive performance.

There are two types of cross validations can be performed: leave one out and k fold [84]. The former one is a particular case of k-fold, which the value of k is 1. k-fold cross validation is one way to improve over the holdout method. The dataset is divided into k subsets, and the holdout method is repeated k times. Each time, one of the k subsets is used as the test set and the other k -1 subsets are put together to form a training set. Then the average error across all k trials is computed. Every data point gets to be in a test set exactly once and gets to be in a training set $k - 1$ times. The variance of the resulting estimate is reduced as k is increased. The advantage of this method is that it matters less how the data gets divided. The disadvantage of this method is that the training algorithm has to be rerun from scratch k times, which means it takes k times as much computation to make an evaluation. A variant of this method is to randomly divide the data into a test and training set k different times. The advantage of doing this is that we can independently choose how large each test set is and how many trials you average over.

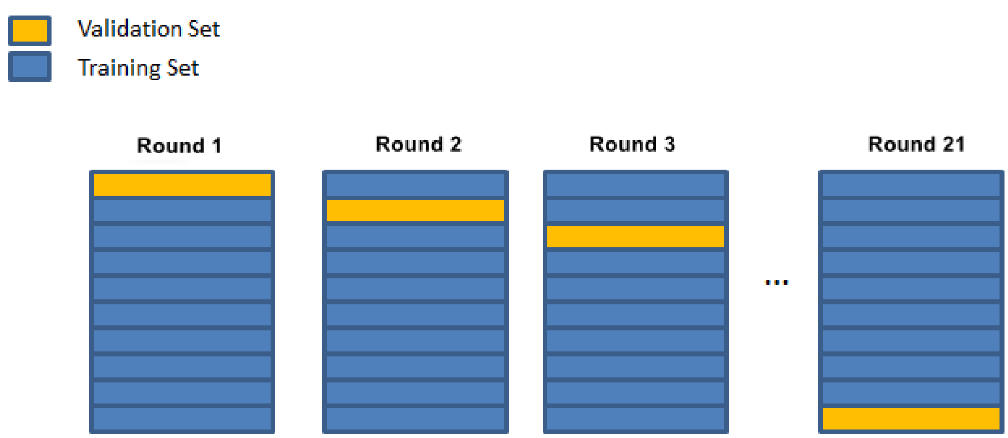

Figure 4-31 Cross validation for a comprehensive dataset

In our case, there are 21 datasets and leave one out cross validation is applied to evaluate the prediction accuracy. A comparison of the original CF and the predicted CF are shown in the following table. In total, there are two datasets are not predicted with the same CF range, which is 2 out of 21, the accuracy is 90.4%。

If more datasets are used for training the decision three, the structure of the decision tree may change a bit, but the prediction should not be affected that much. The three different features are all applied to classify the CF range, the key issue is that the decision tree is evaluating which feature is splitting the data in a best way and arrange the sequence.

4.6.5 The Extendibility of the Prediction System

(1) Additional features

So far there are three features have been applied for CF evaluation, which is extracted from the motion of the catheter tip during radiofrequency ablation, in the future research more features can be added if they are more demonstrated to relate to CF evaluation.

(2) Multi-Class Decision Tree

The mechanism for multiclass classification is based on “One VS One”, if there are N classes for the outputs, there would be N*(N-1)/2 decision trees required. A combination of two different classes needs one decision tree to take care of. In our study, since the amount the classes are fixed, which is 4, so the decision tree needed is always 6, but if there are more features added to evaluate CF, then each decision tree needs to be updated. How to assign the attributes to split the data for getting the CF output range should be recalculated.

(3) Database update for setting range

The boundary value of the ranges is necessary for predicting the CF. The computed parameter such as 3D average distance, 2D ratio, and 1D cost are just certain numbers, how to convert them into a specific range is significant for prediction.

Previously the range was set using the information from eight patients. If possible, more patients can be involved to make the data more comprehensive. The data can be extracted from the patient who need to have the radiofrequency ablation procedure or can be taken from the taken point during the mapping procedure. The information extracted from the patients can be added into the database for updating the range boundary values.

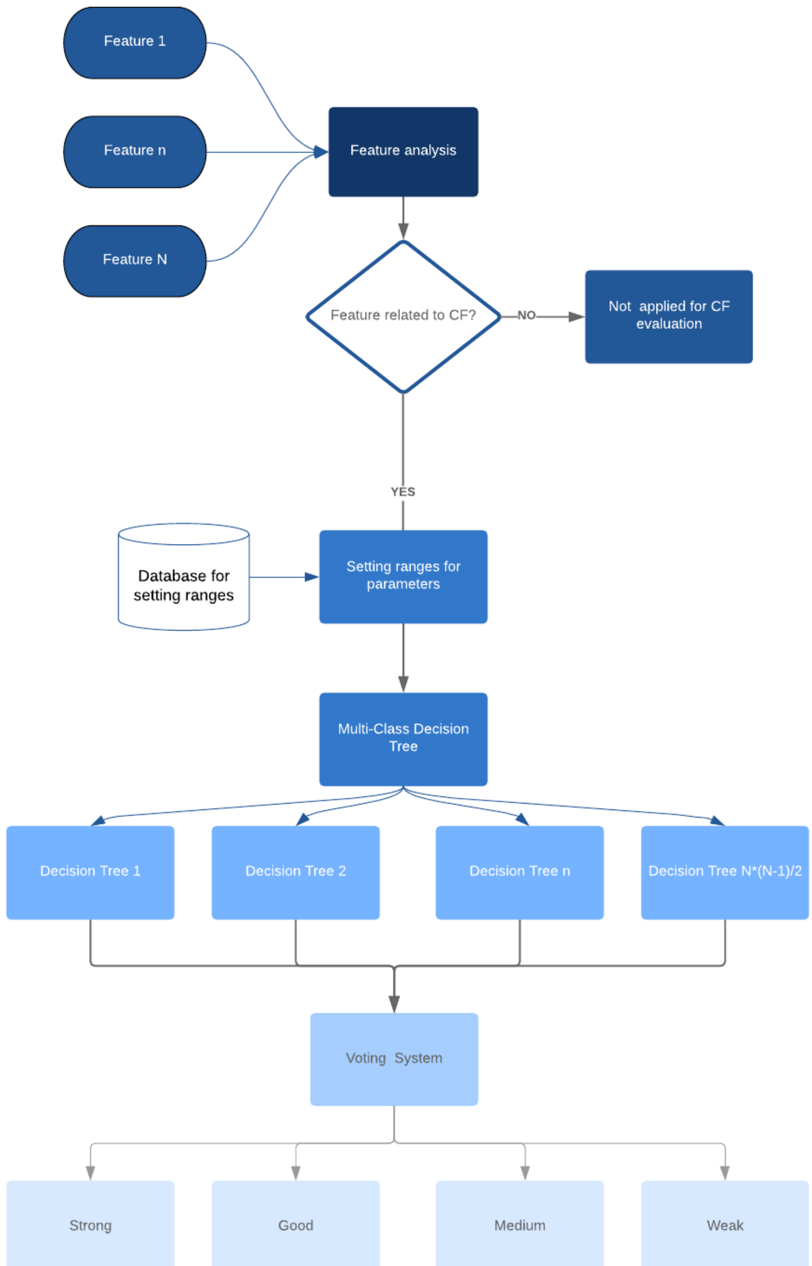

Figure 4-31 The extendibility of the prediction system

4.6 Summary

This Chapter describes the feature extraction using the moving pattern of the catheter tip, based on the location of the catheter tip in the 3D space, plane fitting, primary components analysis and one-dimensional time series similarity are analyzed and further applied for CF evaluation.

A CF predicting system based on decision tree is adopted to combine all the different features and decide for predicting the CF, a comprehensive dataset with the measured CF as reference is taken to test the CF evaluating system, and it is demonstrated to able to obtain the exact result we want if the CF is set into ranges instead of consecutive values.

CHAPTER 5 Intracardiac Electrogram Data Analysis

The relation between the moving pattern of the catheter tip and the electrode-tissue has been discussed in the previous Chapter. As an additional information for CF estimation, the characteristics of the electrogram can be very effective surrogates for CF evaluation during the pre-ablation process, moreover, it also reveals useful information during the ablation process, which is a very good supplement for cardiac contact force evaluation.

5.1 Intracardiac Electrogram Data Description

Electrocardiography is the process of recording the electrical activity of the heart using different electrodes placed on different body parts during a certain period [31]. Thus, the magnitude of the electrogram and information of the electrical depolarization can be obtained during a certain period of time.

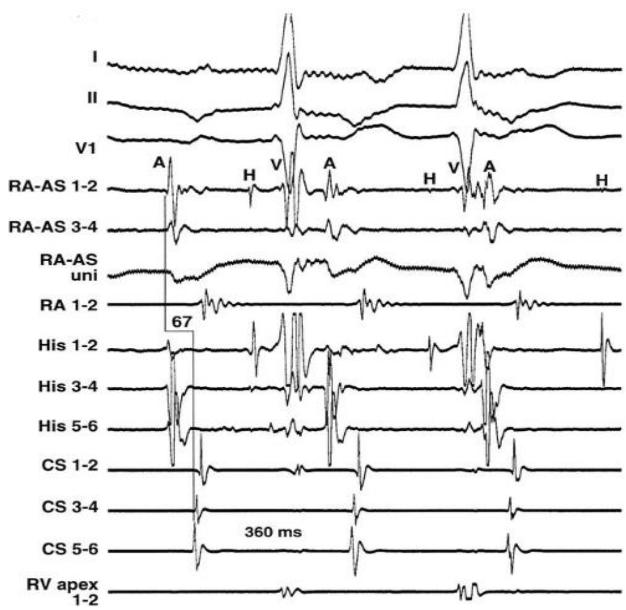

Figure 5-1 An intracardiac electrogram record. Image form "Focal Atrial Tachycardia Originating from the Non-Coronary Aortic Sinus"

There was research to evaluate CF by using the morphology of the electrogram. Kumar et, al [62] propose a study to evaluate CF using several features such as EGM amplitude. Based on their study, the correlation between CF and features extracted from electrogram quality is not effective to predict CF. There could be different reasons, for example, the conductivity of the heart tissue in different locations of the heart chamber may vary, which affect the magnitude of the electrogram. Considering there might be better electrical coupling if there is stronger electrode-tissue contact, I analyze the data based on the frequency domain in my dissertation.

5.2 The idea of electrogram comparison

The general idea of using the electrogram characteristics is electrogram comparison of different electrodes. The electrical coupling between the electrode and tissue relates to the contact. In this study, we assume a stronger electrode-tissue contact may bring a better electrical coupling for the ablation catheter. By comparing with a stable signal obtained from another catheter, the contact condition of the ablation catheter is analyzed.

5.2.1 Electrogram comparison

The electrograms collected from the ablation catheter and the reference catheter are compared to evaluate the ablation catheter contact. The reference point taken in our study is Cs p electrode from the coronary sinus (Cs) catheter. The coronary sinus lies between the left atrium and left ventricle on the posterior side of the heart [1]. When a catheter is placed in this location, activation of both the left atrium and the left ventricle can be visualized. What is more, the Cs catheter sticks to the wall of coronary sinus all the time tightly, thus, the electrogram collected from Cs catheter electrodes normally are very good. Considering there might be better electrical coupling if there is better electrode-tissue contact, our study focuses on analyzing the data based on the frequency domain. In the beginning, a spectral analysis of the electrogram is presented, the signal from the reference point and the ablation point are applied to make a comparison. The general idea is the major frequency of the spectral domain should be similar when the tissue-electrode contact is strong.

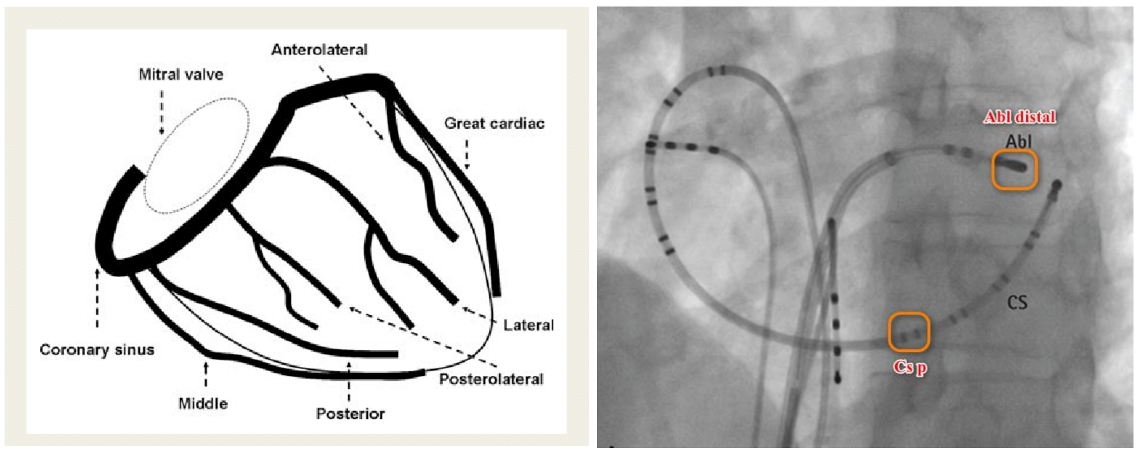

(A) (B)

Figure 5-2 (A)The coronary sinus lies between the left atrium and left ventricle on the posterior side of the heart. (B)The Cs catheter and ablation catheter showing in the fluoroscopy image.

5.2.2 Fast Fourier transform

Fast Fourier transform (FFT) [81,82] is a fast-computational algorithm for the discrete Fourier transform (DFT), it is a process of taking an array of time domain waveform samples, to produce a new array of frequency domain spectrum samples. Suppose the input array in the time domain is a duration T_d seconds and it has N samples, then the frequency interval and sampling frequency are ΔT and f_s respectively.

$$\Delta T = T_{\mathrm{d}} / N \tag{5.1}$$

$$f_s = 1/\Delta T \tag{5.2}$$

The number of the samples on the input is exactly the same as the number of samples on the output, which is N samples in the frequency domain as well. Suppose the span of frequency domain is Bb which stands for bi-directional bandwidth, the sampling interval and sampling frequency in the frequency domain is Δf and

$$B_b = f_s \tag{5.3}$$

$$\Delta f = B_b / N = f_s / N \tag{5.4}$$

N must be a power of 2 for FFT algorithm be truly fast. In the study, intracardiac electrical signals come from 16 channels are documented in real time during diagnostic and therapeutic procedures. What we can see from the monitoring system is the analog signal. In the EGM recording system data is saved in the digital form. The sampling frequency is 1000 HZ.

5.2.3 Kolmogorov-Smirnov test

The Kolmogorov-Smirnov test (KS test) is a statistical hypothesis test used to check if two datasets differ significantly. There is no need to make assumption about the data distribution using KS test [83]. Generally speaking, it is non-parametric and distribution free as well. At the beginning, a null hypothesis H0, needs to be set. Which is we assume the two samples coming from the same distribution. The alternative hypothesis H1, can be claimed as the two samples from different distributions. Suppose the two samples we are testing have empirical cumulative distribution functions $F_n(x)$ and $G_m(x)$, By using KS test, the test statistic can be obtained for analysis. For instance, the maximum absolute difference between $F_n(x)$ and $G_m(x)$ which is called D, is used to determine if two datasets differ significantly.

$$D = \sup_{-\infty<x<\infty} |F_n(x) - G_m(x)| \tag{5.5}$$

In the study, data collected in one situation (reference point) is compared to data collected in a different situation (ablation point) with the aim of seeing if there is a significant difference between the two distributions. The resource comes from the spectral data processed using FFT, the spectral data is normalized to form the discrete sequence, then KS test is applied to do the analysis.

5.3 Analysis and results

In the clinical study, there are 32 points taken in total before the catheter ablation procedure, most of the points are collected from the left atrium. For each point, the EGM's from all the 16 different channels are recorded. What we focus is the signal from the distal electrode of ablation catheter (Abl d), the proximal electrode of the Cs catheter (Cs p), which is known as the reference point, the signal collected from Cs p is very stable due to the tight contact with the tissue. For each point, the time domain of those two electrodes is processed by FFT, to generate the frequency domain array. The magnitude of the two arrays could be very different, normalization needs to be applied to guarantee the input for the KS test does not interfere.

5.3.1 FFT processing

FFT processing transforms the signal from time domain to frequency domain. The sampling frequency from the time domain is 1000 HZ. Thus, the bi-directional bandwidth is equal to that, considering symmetry of the frequency domain, the frequency range showing up in the frequency domain is 0 to 500 HZ.

Figure 5-3(A) shows the time domain of a specific point, from which we can see the signal collected from two electrodes are very similar. Normally when there is strong contact between the ablation electrode and tissue, the signal frequency is similar to the reference point. Figure 5-3 (B) shows the frequency domain of the dataset after FFT, which clearly presenting the comparison of the two spectral graphs, the dominant frequency band basically is the same.

the distribution of the FFT output can be compared using KS test, considering the distributions are in the form of discrete histogram, it can be taken as the two arrays for the input of the KS test after normalization. The comparison will be talked about later.

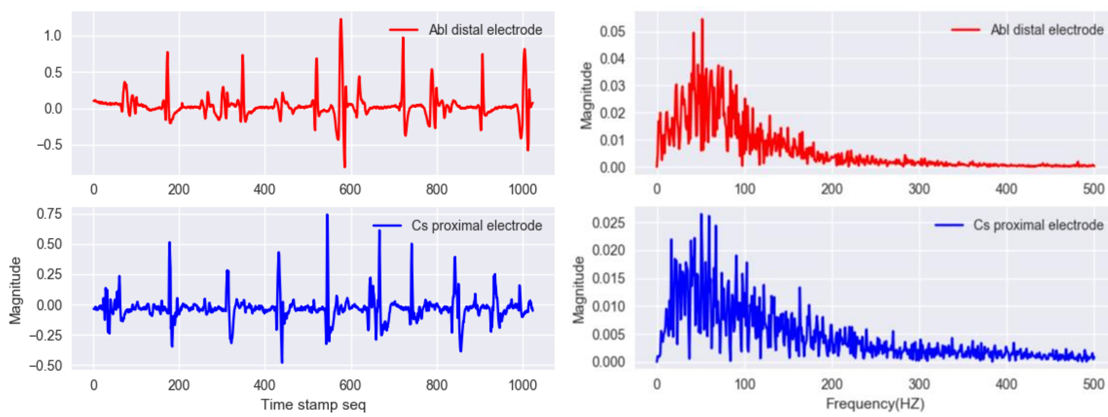

(A) (B)

Figure 5-3 One taken point from the clinical study. CF:27g, location: upper left ventricle. (A)The graph above shows the signal of the time domain from the distal electrode of the ablation catheter. The graph below shows the corresponding graph from the reference point, which is the signal from the proximal electrode of the CS catheter. (B). The corresponding spectral graph. The figure above shows the spectral graph of the electrogram signal from the distal electrode of the ablation catheter. The figure below, shows the corresponding graph from the reference point, which is the signal from the proximal electrode of the CS catheter.

The signal from the proximal electrode of the ablation catheter may provide some information about the orientation of the catheter tip. Abl p electrode is further away from the tip compared with the Abl d electrode, thus, when it receives regular signal, normally it means the whole catheter tip attaches the tissue. Though it cannot be analyzed for contact force evaluation, the information is still valuable for checking the orientation.

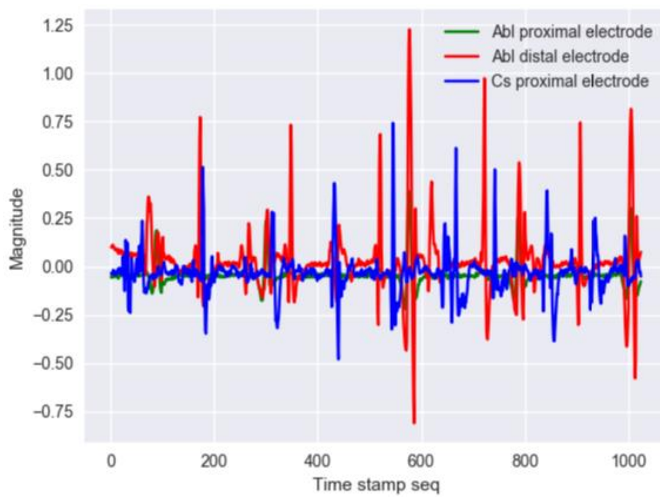

Figure 5-4 The signal of the time domain collected from CS p, Abl d, Abl p electrodes respectively, Abl p may tell some information about the orientation of the catheter tip

The contact level affects the electrical coupling, in the study, there are also different points with low contact force, or no contact force collected for comparison. Figure 5-5(A)(B) shows the time domain and frequency domain of a weak contact force for a taken point, obviously, the mode of the spectral data is very different.

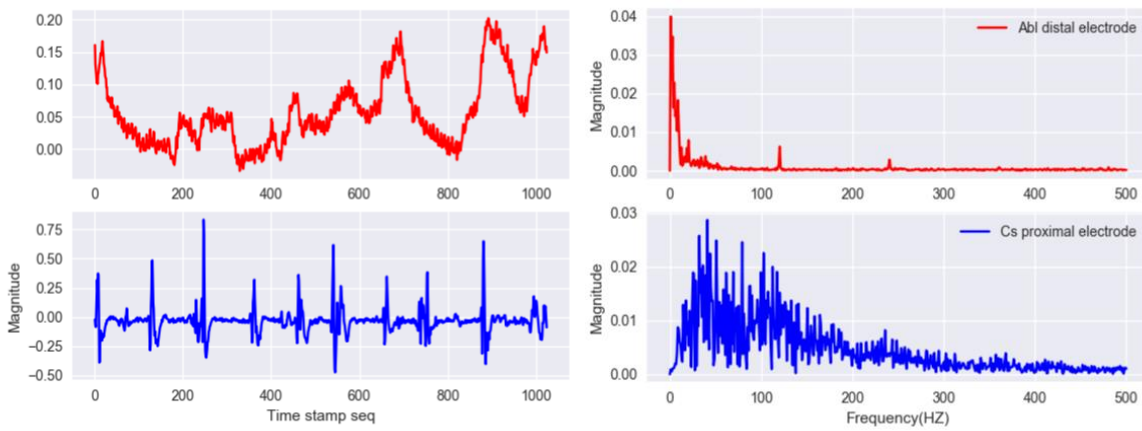

(A) (B)

Figure 5-5 One taken point from the clinical study. The signal from the time domain, CF:3g, location: upper left ventricle. (A)Data from time domain with weak contact force, the signal collected from time domain is irregular without a clear pattern. (B) Spectral data after FFT, CF:3 g, location: upper left ventricle. The spectral difference demonstrates that the mode of the signals collected from the two electrodes are very different.

5.3.2 KS test analysis

In the implementation, a D statistic and a p-value are returned by the KS test, the p-value is related to the D value which can be calculated. The D statistic is the absolute max distance between the two CDFs [83]. If this value is closer to 0, it means more likely the two datasets are from the same distribution, on the contrary, they are probably from different distributions.

The null hypothesis H0 is rejected at a significance level α if

$$D > c(\alpha)\sqrt{\frac{n+m}{nm}} \tag{5.6}$$

The value of α and c(α) is provided below, n and m are the sample size for two different datasets respectively.

α	**0.10**	**0.05**	**0.025**	**0.01**	**0.005**	**0.001**
$c(\alpha)$	1.22	1.36	1.48	1.63	1.73	1.95

Table 5-1 The value of $c(\alpha)$ for the most common levels of α

The KS test can be classified as one-sample test and two-sample test. The first one quantifies the distance between the CDF of the reference distribution and the empirical distribution function of the sample dataset, while the two-sample test is between the empirical distribution functions of two samples. The KS two-sample test is sensitive to the differences in both the shape and the position of the empirical CDFs for the two sample datasets.

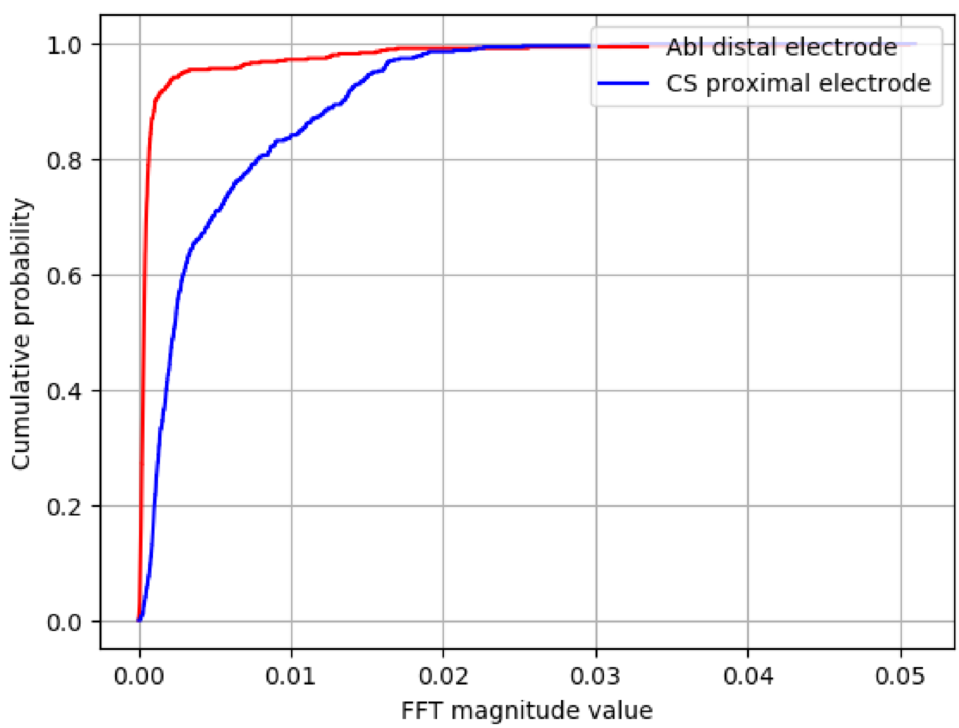

Figure 5-6 CF:1g, D statistic: 0.74, p-value: 4.25e-18. location: left atrium. K-S test for one of the taken points during catheter ablation, the D statistic can be extracted by finding the biggest vertical distance, which also presents the difference between the distributions collected from two different electrodes.

The major frequency of the spectral domain collected from the reference point (Cs p) and the test point (Abl d) should be similar when the tissue-electrode contact is strong, which means probably is from the same distribution. Otherwise, the two distribution differs. Thus, the null hypothesis H0 is that the two samples (spectral data) we are testing come from the same distribution. If the likelihood of the samples being from different distributions exceeds a confidence level we demand the original hypothesis is rejected in favor of the hypothesis, H1, that the two samples are from different distributions, which means the contact force is weak.

The decision to reject the null hypothesis is based on the p-value computed for the dataset, which we defined as if the contact force is strong. Before performing the test, the significance level for the problem is set.

5.3.3 The Relation of 1D Data and Catheter CF

Based on the data collected in the clinical study, checking the electrogram frequency domain is a proper way to evaluate the contact level between the electrode and tissue, the reference point which is the pivot of the comparison takes an important role in this method, picking up the Cs p electrode benefits from the stable contact between the electrode and tissue.

The frequency domain comparison method can be significant for determining if the electrode-tissue contact is strong or weak, but it is hard to define or quantize the contact force level, so far there is no way to find the proportional relation of the contact force and frequency comparison statistics. The electrogram information can be applied as the independent factor to do the analysis but can also be combined with other surrogates to define the contact force level, more work needs to be done for quantizing the amount of the contact force during catheter ablation using different surrogates. What is more, the limitation lays on electrogram is only suitable for the pre-ablation process. Suppose the tissue is ablated, the contact force does not matter to the signal collection anyway, cause the tissue is burned and might be impossible for the electrical coupling. For comparing the frequency domain difference, the Kolmogorov–Smirnov test does not provide any confidence intervals, some other tests might be better suited if confidence intervals are required [83].

If simply set the boundary for distinguishing contact force strength at 10 g, by using KS test to check if the spectral data differ, after normalization, further to examine if the contact force is strong, 25 out of 32 points can be correctly predicted, which the classification accuracy is 78.5%.

CHAPTER 6 Discussion and Future Work

This Chapter is a review of the research objectives and results. I will emphasize the scientific contributions that this research has achieved. In the end, some prospective points for the future work of this research are discussed.

6.1 Summary

In this dissertation, we focused on estimating the electrode-tissue contact force during catheter ablation. Different features extracted from the motion of the catheter tip are analyzed, furthermore, the extracted features are combined using machine learning algorithm to evaluate the contact force.

Considering a catheter tip keeps moving during catheter ablation, if the position of the catheter tip can be recorded, then the motion of the catheter tip can be tracked and analyzed. Based on the clinical study data, we assume that the moving pattern is more regular when there is stronger contact between the tissue and catheter tip, on the contrary, the contact force might be weaker if the moving pattern is more random.

As was discussed in the statement of the research, this work is split into two distinct sections, one dealing with the contact force evaluating mechanism which is based on a decision tree (Chapter 3) and one dealing with feature selection and analysis (Chapter 4). Essentially the CF evaluating mechanism is based on machine learning, there are different algorithms work for the evaluation mechanism, considering the data size and the output range, we pick up decision tree to organize all the features to make a comprehensive contact force evaluation. For building the decision tree, there is an attribute condition test applied on each non-terminal node. Basically, each node represents a test performed on a single attribute and go left or right depending on the result of the test. Then keep traversing the tree until reaching a leaf node which contains the class prediction. By going through the decision tree using all the features information, we can make a comprehensive evaluation of the electrode-tissue contact force.

The objective of our research is to pursue the contact detection accuracy and lower the cost would benefit the application of the CF sensing. In Chapter 2, there is a discussion of using different methods to measure contact force including direct and indirect way, the direct measuring based on physical touching is very effective but very expensive, catheters are placed with delicate sensors, as well as a sophisticated structure, which makes them a high cost. As for indirect measurement, there are different problems for achieving certain level of accuracy. Thus, based on our work, it is significant to make a good balance between controlling cost and estimating accuracy.

6.2 Conclusion

In this dissertation, we have made some contributions to estimate the electrode-tissue contact force. Now, we will summarize our main contributions below.

First of all, this is the first work to explore the association between the contact force and the moving pattern of the catheter tip during catheter ablation. Before this dissertation, researchers tried to solve this problem based on different mechanisms, but none of them deeply examined the catheter tip motion. Based on our observation from the clinical dataset collected, the moving pattern of the catheter tip is different when the electrode-tissue contact force level varies. Thus, the features of the catheter tip moving pattern are significant for the contact force estimation. In my dissertation, 3D data is obtained using two different views via the back-projection method. Based on the 3D data, 2D and 1D data are also extracted and analyzed to describe the difference when the contact force level varies. Normally, if the contact force is strong, there is a high possibility that all the points gathered tight fitting on one plane, and the projection of the 2D data and 1D data have different characteristics, the results from Chapter 4 also explain that.

Secondly, the dissertation is also the first time where the frequency domain analysis of the electrogram is used to estimate contact force. In my dissertation, it is an auxiliary method applied for evaluating contact force. Previously the quality of the electrogram is discussed for evaluating CF, based on their study, the correlation between CF and features extracted from electrogram quality is not effective to predict CF. Considering there might be better electrical coupling if there is better electrode-tissue contact, I try to analyze the data based on the frequency domain. The general idea is the electrograms collected from the ablation catheter and the reference catheter are compared to evaluate the ablation catheter contact. The coronary sinus lies between the left atrium and left ventricle on the posterior side of the heart. When a catheter is placed in this location, it is always very stable. Thus, it provides good electrical coupling information for our study.

6.3 Limitations

There are some limitations of our data collection and result analysis. One of these comes from the data size in the clinical study. To get the contact force data, it brings extra work during the ablation procedure, so basically, there is no way to get the big data to do the analysis, which also limits the ways to make analysis. The other one comes from the CF measuring. Though CF monitoring has been proved that it makes the ablation procedure safer and more efficient, which can also cause less exposure time for both patient and physician, but there is also discussion about the limitation of CF monitoring. First of all, the optimal CF value may change depending on the position in the chamber, the characteristics of the tissue and so on, what is more, the approaching angle and the blood flow also matter to the effect of ablation. Okumura mentions in his research that the optimal CF value may vary between mapping and ablation procedure as well [36]. Secondly, CF keeps changing periodically due to cardiac and respiratory cycles even when sticking to tissue in the chamber [37]. the value of CF can be presented in a different form such as peak value, the mean value and force-time integral (FTI). The previous study has shown that the ablation lesion size was correlated linearly to force time integral, not to peak CF value [38]. Several studies also examined the relationship between CF and complications such as perforation and steam pop [38]. The safety of catheter ablation definitely is an important issue, except for CF, there are many other factors involved in such complications, such as ablation position, tissue characteristics, blood flow and so on.

6.4 Future work

This section briefly describes some interesting topics in this research, which are worth investigating further. Although the provided analyses and methodologies are quite good and constitute a set of powerful tools to guarantee the real-time CF estimation, there are some improvements that can still be made. Under this context, I will survey some of the provided results which can be improved or extended further. Here are these points:

- Exploring new features based on catheter tip motion to evaluate contact force. In my dissertation, there are several features: 3D, 2D, 1D position of the catheter tip are applied to build the relationship between the contact force and some statistics. considering the characteristics of the catheter tip motion, the features are closely related to the accuracy of the contact force evolution while the algorithm directly affects the evolution result. If there is an obvious difference between different tip moving features, CF evaluating algorithm should not be very complicated, on the contrary, data description and evaluating algorithm need more work.

- It could be interesting to check the relationship between electrode-tissue contact using electrical coupling information. Here I use the word “contact” instead of “contact force”, the Contact force is a very concrete way to describe the tightness between tissue and catheter tip, but considering there are different factors influencing contact force, such as the angle of approaching, the blood flow. So, I think it is significant to redefine contact during catheter ablation.
- Combine the motion of the catheter tip and electrogram characteristics to evaluate the CF. So far, the electrogram is only applied for pre-ablation contact force evaluation, one reason is that we don’t know if the weak electrical coupling is caused by weak electrode-tissue contact or the tissue is ablated. By combing the information of the catheter tip location, we can try to locate if the ablation catheter is in position or not, later making a further evaluation for the CF using the electrogram characteristics.

BIBLIOGRAPHY

[1] Iaizzo, Paul A., ed. Handbook of Cardiac Anatomy, Physiology, and Devices. Springer Science & Business Media, 2009.

[2] Addetia, Karima, et al. "Simultaneous longitudinal strain in all 4 cardiac chambers: a novel method for comprehensive functional assessment of the heart." *Circulation: Cardiovascular Imaging* 9.3 (2016): e003895.

[3] Fox, Stuart Ira. Human Physiology 9th ed. McGraw-Hill Press, New York, USA, 2006.

[4] Hine, Robert, and Elizabeth Martin, eds. A Dictionary of Biology. Oxford Quick Reference, 2015.

[5] Pratt, Rebecca. "Cardiovascular System: Blood." In Anatomy One, Amirsys, Inc. Salt Lake City, Utah (2000).

[6] Moorman, Antoon FM, et al. "Development of the cardiac conduction system." *Circulation Research* 82.6 (1998): 629-644.

[7] Nattel, Stanley, et al. "New directions in cardiac arrhythmia management: present challenges and future solutions." *Canadian Journal of Cardiology* 30.12 (2014): S420-S430.

[8] Tse, Gary. "Mechanisms of cardiac arrhythmias." *Journal of Arrhythmia* 32.2 (2016): 75-81.

[9] Fischer, Avi. "Arrhythmias: Supraventricular tachycardias, ventricular tachycardias and bradyarrhythmias." Essentials of Hospital Medicine: A Practical Guide for Clinicians. 2013. 247-258.

[10] Bunch, T. Jared, and Michael J. Cutler. "Is pulmonary vein isolation still the cornerstone in atrial fibrillation ablation?." *Journal of Thoracic Disease* 7.2 (2015): 132.

[11] Mozaffarian, Dariush, et al. "Executive summary: heart disease and stroke statistics-2016 update: a report from the American Heart Association." *Circulation* 133.4 (2016): 447-454.

[12] Bhaumik, Asish, et al. "A review on cardiac arrhythmia and cardiac ablation: Invasive techniques and future perspective." *World Journal of Pharmaceutical and Medical Research* 2 (2016): 105-111.

[13] Swartz, John F., et al. "Process and device for the treatment of atrial arrhythmia." U.S. Patent No. 5,938,660. 17 Aug. 1999.

[14] Morillo, Carlos A., et al. "Radiofrequency ablation vs antiarrhythmic drugs as first-line treatment of paroxysmal atrial fibrillation (RAAFT-2): a randomized trial." *JAMA* 311.7 (2014): 692-700.

[15] Haissaguerre, Michel, et al. "Successful catheter ablation of atrial fibrillation." *Journal of Cardiovascular Electrophysiology* 5.12 (1994): 1045-1052.

[16] Kühne, Michael, et al. "Cryoballoon versus radiofrequency catheter ablation of paroxysmal atrial fibrillation: biomarkers of myocardial injury, recurrence rates, and pulmonary vein reconnection patterns." *Heart Rhythm* 7.12 (2010): 1770-1776.

[17] Wazni, Oussama M., et al. "Embolic events and char formation during pulmonary vein isolation in patients with atrial fibrillation: impact of different anticoagulation regimens and importance of intracardiac echo imaging." *Journal of Cardiovascular Electrophysiology* 16.6 (2005): 576-581.

[18] Courtney M. Townsend. Sabiston Textbook of Surgery: The Biological Basis of Modern Surgical Practice, 19th ed. Philadelphia, PA: Elsevier Saunders. p. 236.

[19] Akca, Ferdi, et al. "A prospective study on safety of catheter ablation procedures: CF guided ablation could reduce the risk of cardiac perforation." *International Journal of Cardiology* 179 (2015): 441-448.

[20] Yokoyama, Katsuaki, et al. "Novel CF sensor incorporated in irrigated radiofrequency ablation catheter predicts lesion size and incidence of steam pop and thrombus" *Circulation: Arrhythmia and Electrophysiology* 1.5 (2008): 354-362.

[21] Simon, Caroline J., et al. "Pulmonary radiofrequency ablation: long-term safety and efficacy in 153 patients." *Radiology* 243.1 (2007): 268-275.

[22] Matsudaira, Kagari, et al. "High incidence of thrombus formation without impedance rise during radiofrequency ablation using electrode temperature control." *Pacing and Clinical Electrophysiology* 26.5 (2003): 1227-1237.

[23] Perna, Francesco, et al. "Assessment of catheter tip CF resulting in cardiac perforation in swine atria using force sensing technologyclinical perspective." *Circulation: Arrhythmia and Electrophysiology* 4.2 (2011): 218-224.

[24] Shah, Dipen, et al. "Catheter tip force required for mechanical perforation of porcine cardiac chambers." *Europace* 13.2 (2011): 277-283.

[25] Gingold, Eric. "Modern fluoroscopy imaging systems." *Image Wisely publicado em* (2014).

[26] Sadick, V., et al. "Impact of biplane versus single-plane imaging on radiation dose, contrast load and procedural time in coronary angioplasty." *The British Journal of Radiology* 83.989 (2010): 379-394.

[27] Fallavollita, Pascal. "The future of cardiac mapping." Cardiac Arrhythmias-New Considerations. InTech, 2012: 213-215

[28] Stabile, Giuseppe, et al. "Reduced fluoroscopy exposure during ablation of atrial fibrillation using a novel electroanatomical navigation system: a multicentre experience." *Europace* 14.1 (2011): 60-65.

[29] Khaykin, Yaariv, et al. "CARTO-guided vs. NavX-guided pulmonary vein antrum isolation and pulmonary vein antrum isolation performed without 3-D mapping: effect of the 3-D mapping system on procedure duration and fluoroscopy time." *Journal of Interventional Cardiac Electrophysiology* 30.3 (2011): 233-240.

[30] Sra, Jasbir, et al. "Identifying the third dimension in 2D fluoroscopy to create 3D cardiac maps." *JCI insight* 1.21 (2016).

[31] Zou, Yao, et al. "An energy-efficient design for ECG recording and R-peak detection based on wavelet transform." *IEEE Transactions on Circuits and Systems II: Express Briefs* 62.2 (2015): 119-123.

[32] Marijon, Eloi, et al. "Real-time contact force sensing for pulmonary vein isolation in the setting of paroxysmal atrial fibrillation: procedural and 1-year results." *Journal of Cardiovascular Electrophysiology* 25.2 (2014): 130-137.

[33] Shurrab, Mohammed, et al. "Impact of contact force technology on atrial fibrillation ablation: a meta-analysis." *Journal of the American Heart Association* 4.9 (2015): e002476.

[34] Matía Francés, Roberto, et al. "Characterization of the impact of catheter–tissue contact force in lesion formation during cavo-tricuspid isthmus ablation in an experimental swine model." *Europace* 16.11 (2013): 1679-1683.

[35] Providência, Rui, et al. "Higher contact-force values associated with better mid-term outcome of paroxysmal atrial fibrillation ablation using the SmartTouch™ catheter." *EP Europace* 17.1 (2015): 56-63.

[36] Okumura, Yasuo, et al. "A systematical analysis of in vivo contact forces on virtual catheter tip/tissue surface contact during cardiac mapping and intervention." *Journal of Cardiovascular Electrophysiology* 19.6 (2008): 632-640.

[37] Mizuno, Hiroya, Giuseppe Maccabelli, and Paolo Della Bella. "Possibility of contact force monitoring during catheter ablation of ventricular tachycardia." *Interventional Cardiology* 4.6 (2012): 701-708.

[38] Afzal, Muhammad R., et al. "Use of contact force sensing technology during radiofrequency ablation reduces recurrence of atrial fibrillation: A systematic review and meta-analysis." *Heart Rhythm* 12.9 (2015): 1990-1996.

[39] Kerst, Gunter, et al. "Contact force–controlled zero-fluoroscopy catheter ablation of right-sided and left atrial arrhythmia substrates." *Heart Rhythm* 9.5 (2012): 709-714.

[40] Green, C. E., and M. J. Kelley. "A renewed role for fluoroscopy in the evaluation of cardiac disease." *Radiologic Clinics of North America* 18.3 (1980): 345-357.

[41] Lin, Tina, et al. "Thermocool® Smartouch® catheter–The evidence so far for contact force technology and the role of Visitag™ Module." *Arrhythmia & Electrophysiology Review* 3.1 (2014): 44.

[42] Page, Stephen P., and Mehul Dhinoja. "SmartTouch™—The emerging role of contact force technology in complex catheter ablation." *Arrhythmia & Electrophysiology Review* 1.1 (2012): 59.

[43] Natale, Andrea, et al. "Paroxysmal AF catheter ablation with a contact force sensing catheter: results of the prospective, multicenter SMART-AF trial." *Journal of the American College of Cardiology* 64.7 (2014): 647-656.

[44] Lee, Geoffrey, et al. "Use of a contact force-sensing ablation catheter with advanced catheter location significantly reduces fluoroscopy time and radiation dose in catheter ablation of atrial fibrillation." *EP Europace* 18.2 (2016): 211-218.

[45] Govari, Assaf, et al. "Catheter with pressure sensing." U.S. Patent No. 8,357,152. 22 Jan. 2013.

[46] Stabile, Giuseppe, et al. "Catheter–tissue contact force for pulmonary veins isolation: a pilot multicentre study on effect on procedure and fluoroscopy time." *Europace* 16.3 (2014): 335-340.

[47] Ullah, Waqas, R. J. Schilling, and T. Wong. "Contact force and atrial fibrillation ablation." *Journal of Atrial Fibrillation* 8.5 (2016).

[48] Black-Maier, Eric, et al. "Risk of atrioesophageal fistula formation with contact force–sensing catheters." *Heart Rhythm* 14.9 (2017): 1328-1333.

[49] Sacher, Frederic, et al. "Endocardial versus epicardial ventricular radiofrequency ablation: utility of in vivo contact force assessment." *Circulation: Arrhythmia and Electrophysiology* 6.1 (2013): 144-150.

[50] Kuck, Karl-Heinz, et al. "A novel radiofrequency ablation catheter using contact force sensing: Toccata study." *Heart Rhythm* 9.1 (2012): 18-23.

[51] Reddy, Vivek Y., et al. "The relationship between contact force and clinical outcome during radiofrequency catheter ablation of atrial fibrillation in the TOCCATA study." *Heart Rhythm* 9.11 (2012): 1789-1795.

[52] Thiagalingam, Aravinda, et al. "Impedance and temperature monitoring improve the safety of closed-loop irrigated-tip radiofrequency ablation." *Journal of Cardiovascular Electrophysiology* 18.3 (2007): 318-325.

[53] Haissaguerre, M., et al. "Relation between impedance and endocardial contact during radiofrequency catheter ablation." *American Heart Journal* 128.2 (1994).

[54] Zheng, Xiangsheng, et al. "Electrode impedance: an indicator of electrode-tissue contact and lesion dimensions during linear ablation." *Journal of Interventional Cardiac Electrophysiology* 4.4 (2000): 645-654.

[55] Cao, Hong, et al. "Using electrical impedance to predict catheter-endocardial contact during RF cardiac ablation." *IEEE Transactions on Biomedical Engineering* 49.3 (2002): 247-253.

[56] Reichlin, Tobias, et al. "Initial impedance decrease as an indicator of good catheter contact: insights from radiofrequency ablation with force sensing catheters." *Heart Rhythm* 11.2 (2014): 194-201.

[57] Reichlin, Tobias, et al. "Feasibility, efficacy, and safety of radiofrequency ablation of atrial fibrillation guided by monitoring of the initial impedance decrease as a surrogate of catheter contact." *Journal of Cardiovascular Electrophysiology*26.4 (2015): 390-396.

[58] De Bortoli, Alessandro, et al. "Ablation effect indicated by impedance fall is correlated with contact force level during ablation for atrial fibrillation." *Journal of Cardiovascular Electrophysiology* 24.11 (2013): 1210-1215.

[59] Stern, Roger A., and Jerome Jackson. "Cardiac ablation systems and methods using tissue temperature monitoring and control." U.S. Patent No. 5,743,903. 28 Apr. 1998.

[60] Govari, Assaf, Christopher Thomas Beeckler, and Athanassios Papaioannou. "Sensing contact of ablation catheter using differential temperature measurements." U.S. Patent No. 8,668,686. 11 Mar. 2014.

[61] Wang, Huisun, Hong Cao, and Jeremy D. Dando. "Ablation catheter electrode having multiple thermal sensors and method of use." U.S. Patent No. 8,460,285. 11 Jun. 2013.

[62] Kumar, Saurabh, et al. "Catheter-tissue CF determines atrial electrogram characteristics before and lesion efficacy after antral pulmonary vein isolation in humans." *Journal of Cardiovascular Electrophysiology* 25.2 (2014): 122-129.

[63] Ullah, Waqas. Factors affecting catheter contact in the human left atrium, its impact on the electrogram and radiofrequency ablation. Diss. Queen Mary University of London, 2015.

[64] Avitall, Boaz, et al. "The effects of electrode-tissue contact on radiofrequency lesion generation." *Pacing and Clinical Electrophysiology* 20.12 (1997): 2899-2910.

[65] Ikeda, Atsushi, et al. "Relationship between catheter contact force and radiofrequency lesion size and incidence of steam pop in the beating canine heart: electrogram amplitude, impedance, and electrode temperature are poor predictors of electrode-tissue contact force and lesion size." *Circulation: Arrhythmia and Electrophysiology* 7.6 (2014): 1174-1180.

[66] Shah, Dipen C., et al. "Area under the real-time contact force curve (force–time integral) predicts radiofrequency lesion size in an in vitro contractile model." *Journal of Cardiovascular Electrophysiology* 21.9 (2010): 1038-1043.

[67] Squara, Fabien, et al. "Contact force and force-time integral in atrial radiofrequency ablation predict transmurality of lesions." *Europace* 16.5 (2014): 660-667.

[68] Ho, Siu Chun Michael, et al. "FBG sensor for contact level monitoring and prediction of perforation in cardiac ablation." *Sensors* 12.1 (2012): 1002-1013.

[69] Mahapatra, Srijoy, et al. "Incidence and predictors of cardiac perforation after permanent pacemaker placement." *Heart Rhythm* 2.9 (2005): 907-911.

[70] Agarwal, Kishan C., et al. "Cardiac perforation from central venous catheters: survival after cardiac tamponade in an infant." *Pediatrics* 73.3 (1984): 333-338.

[71] Neuzil, Petr, et al. "Electrical reconnection after pulmonary vein isolation is contingent on contact force during initial treatment: results from the EFFICAS I study." *Circulation: Arrhythmia and Electrophysiology* 6.2 (2013): 327-333.

[72] Kautzner, Josef, et al. "EFFICAS II: optimization of catheter contact force improves outcome of pulmonary vein isolation for paroxysmal atrial fibrillation." *Ep Europace* 17.8 (2015): 1229-1235.

[73] Bourier, Felix, et al. "Pulmonary vein isolation supported by MRI-derived 3D-augmented biplane fluoroscopy: a feasibility study and a quantitative analysis of the accuracy of the technique." *Journal of Cardiovascular Electrophysiology* 24.2 (2013): 113-120.

[74] DeSena, H. C., et al. "Future Diagnostic Strategies—Pediatric." In Cardioskeletal Myopathies in Children and Young Adults, Jefferies et al., ed. Academic Press 2017. 361-379.

[75] Quinlan, J. Ross. "Induction of decision trees." *Machine Learning* 1.1 (1986): 81-106.

[76] Drummond, Chris, and Robert C. Holte. "Exploiting the cost (in) sensitivity of decision tree splitting criteria." *ICML*. Vol. 1. No. 1. 2000.

[77] Murthy, Sreerama K. "Automatic construction of decision trees from data: A multi-disciplinary survey." *Data Mining and Knowledge Discovery* 2.4 (1998): 345-389.

[78] Polat, Kemal, and Salih Güneş. "A novel hybrid intelligent method based on C4. 5 decision tree classifier and one-against-all approach for multi-class classification problems." *Expert Systems with Applications* 36.2 (2009): 1587-1592.

[79] Aly, Mohamed. "Survey on multiclass classification methods." *Neural Net*works 19 (2005): 1-9.

[80] Berndt, Donald J., and James Clifford. "Using dynamic time warping to find patterns in time series." *KDD Workshop*. Vol. 10. No. 16. 1994.

[81] Nussbaumer, Henri J. Fast Fourier transform and convolution algorithms. Vol. 2. Springer Science & Business Media, 2012.

[82] Bergland, G. D. "A guided tour of the fast Fourier transform." *IEEE Spectrum* 6.7 (1969): 41-52.

[83] Massey Jr, Frank J. "The Kolmogorov-Smirnov test for goodness of fit." *Journal of the American Statistical Association* 46.253 (1951): 68-78.

[84] Kohavi, Ron. "A study of cross-validation and bootstrap for accuracy estimation and model selection." Ijcai. Vol. 14. No. 2. 1995.